

# JGR Atmospheres

## RESEARCH ARTICLE

10.1029/2020JD033833

### Key Points:

- Melt ponds must be considered when studying snowball Earth deglaciation
- Snowball Earth deglaciation starts when the annual mean equatorial surface temperature reaches approximately  $-8^{\circ}\text{C}$
- Snowball Earth deglaciation starts from the equator not the subtropical region

### Supporting Information:

- Supporting Information S1
- Movie S1

### Correspondence to:

Y. Liu,  
ygliu@pku.edu.cn

### Citation:

Wu, J., Liu, Y., & Zhao, Z. (2021). How should snowball earth deglaciation start. *Journal of Geophysical Research: Atmospheres*, 126, e2020JD033833.  
<https://doi.org/10.1029/2020JD033833>

Received 3 SEP 2020  
Accepted 4 DEC 2020

### Author Contributions:

**Formal analysis:** Jiacheng Wu, Yonggang Liu  
**Funding acquisition:** Yonggang Liu  
**Investigation:** Yonggang Liu  
**Methodology:** Jiacheng Wu, Yonggang Liu

**Project Administration:** Yonggang Liu

**Resources:** Yonggang Liu

**Software:** Jiacheng Wu, Zhouqiao Zhao

**Supervision:** Yonggang Liu

**Validation:** Jiacheng Wu, Yonggang Liu

**Writing – original draft:** Jiacheng Wu, Yonggang Liu

**Writing – review & editing:** Jiacheng Wu, Yonggang Liu, Zhouqiao Zhao

## How Should Snowball Earth Deglaciation Start

Jiacheng Wu<sup>1</sup> , Yonggang Liu<sup>1</sup> , and Zhouqiao Zhao<sup>1</sup> 

<sup>1</sup>Department of Atmospheric and Oceanic Sciences, School of Physics, Peking University, Beijing, China

**Abstract** The formation of melt ponds is pervasive on sea ice and ice shelves prior to their disintegration. Such process should be critical for the deglaciation of a snowball Earth but has never been considered in previous studies. Here we develop a module to explicitly track the initiation, growth and refreezing of melt ponds on ice. Incorporation of the module into a climate model indicates that it provides a strong positive feedback to the climate. Deglaciation of a snowball Earth will start when the annual mean equatorial surface temperature is only  $-7.7^{\circ}\text{C}$  rather than  $0^{\circ}\text{C}$ . At this point, seasonal melt ponds start to appear in the mid-latitude region. Its positive feedback induces the appearance of perennial melt ponds within the equatorial region and can increase the annual mean temperature there to  $6.1^{\circ}\text{C}$  in less than 10 years. Thus, our results indicate that the threshold  $\text{CO}_2$  required to deglaciate a snowball Earth will be greatly overestimated (by a factor of  $\sim 4$  for the model we use) if the annual mean surface temperature reaching  $0^{\circ}\text{C}$  is used as the criteria. The results also demonstrate unambiguously that the deglaciation of snowball Earth should start from the equator. We then speculate on what will happen to the tropical sea glacier after the surface melting starts.

**Plain Language Summary** The whole Earth was covered by thick ice during a snowball Earth event. When and where the deglaciation of such an event should start have not been answered. Previous studies judged whether atmospheric  $\text{CO}_2$  level was high enough to deglaciate a snowball Earth by checking whether the annual mean surface temperature at the equator approached  $0^{\circ}\text{C}$ . However, seasonal melting of ice must have appeared at a much lower  $\text{CO}_2$  level in the subtropical region where summer is warm. Melt water reduces surface reflectivity and warms the surface, which will induce more melting and form a positive feedback loop. We find that this feedback is very strong; widespread melting occurs once the annual mean equatorial surface temperature approaches  $-8^{\circ}\text{C}$ , much earlier than thought before. Therefore, the threshold  $\text{CO}_2$  level that is required to deglaciate a snowball Earth was greatly overestimated in previous studies. Moreover, our results show that although melt water appears first in the subtropical region during summer, pervasive perennial melt water appears only around the equator due to stable high solar insolation there. This melt water is conjectured to break the thick sea ice near the equator and start the deglaciation of a snowball Earth there.

## 1. Introduction

Once Earth enters a snowball Earth state (e.g., Hoffman et al., 1998, 2017), it is very difficult to recover because the whole globe will be covered by highly reflective snow and ice. Early estimates using energy balance models (EBMs) showed that 0.16–0.29 bar of  $\text{CO}_2$  was required to deglaciate the Neoproterozoic (1,000–541 Ma) snowball Earth (Caldeira & Kasting, 1992; Tajika, 2003). Later studies using general circulation models (GCMs) obtained similar results, i.e., greater than 0.1 bar of  $\text{CO}_2$  was required to initiate the deglaciation (Hu et al., 2011; Le Hir et al., 2007; R. T. Pierrehumbert, 2004). Extremely high  $\text{CO}_2$  level (far greater than 0.2 bar) was required to deglaciate a snowball Earth in the GCM FOAM (Pierrehumbert, 2004, 2005), but it was later identified to be due to a caveat in its cloud parameterization (D. S. J. J. o. C. Abbot, 2014; D. S. Abbot et al., 2012). Nevertheless, the required  $\text{CO}_2$  level to deglaciate a snowball Earth was high. To facilitate the deglaciation, deposition of volcanic dust and other terrestrial dust have been invoked to lower the surface albedo (e.g., D. Li & Pierrehumbert, 2011) or planetary albedo (D. S. Abbot & Halevy, 2010). For the latter, the surface is warmed by the atmosphere, which absorbs large amount of solar insolation due to its high dust loading (Liu et al., 2020). Voluminous dust in the atmosphere or in the ice could lower the threshold  $\text{CO}_2$  level for snowball Earth deglaciation to a range of 0.01–0.1 bar (D. S. Abbot & Halevy, 2010; D. S. Abbot & Pierrehumbert, 2010; Le Hir et al., 2010).

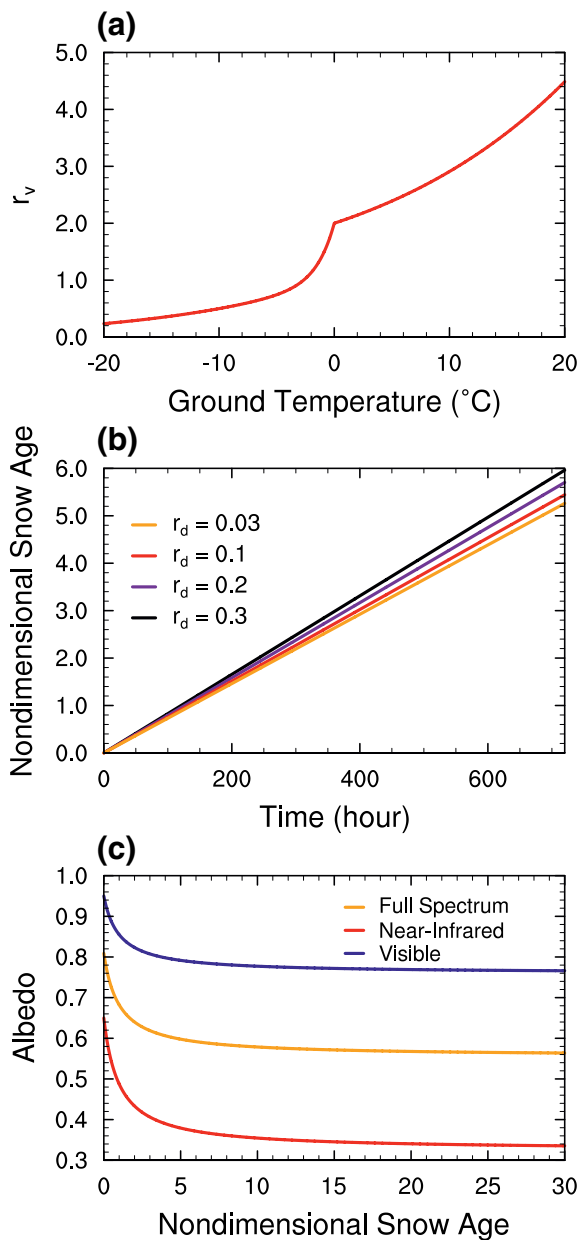


**Figure 1.** Snow aging and its albedo effect. (a) Change of snow-aging parameter  $r_v$  with temperature; (b) growth of non-dimensional snow age with time for different  $r_d$  when temperature is fixed at 0°C and without the change in mass of snow water; (c) change of snow albedo with snow age.

aging was ignored; melt water of snow, if there was any, would likely drip down into deeper snow rather than accumulate at the surface. If snow aging was considered, snow thickness on ice has two contrasting regimes; it was negligible within the equatorial and subtropical latitudinal bands but very thick ( $>0.6$  m) in other regions (see Figure 4d). Therefore, only melt ponds on ice need to be considered. Snow aging is an important process in reducing snow albedo (Le Hir et al., 2010, and reference there) and thus snow thickness, the latter of which pre-conditions the appearance of melt ponds on ice (Figure 3).

The effect of snow aging was unintentionally ignored in the simulations of Hu et al. (2011). The model they used was an atmospheric general circulation model (AGCM), CAM3, coupled to a land surface module,

The start of deglaciation is usually judged by whether the maximum monthly mean (Hu et al., 2011; R. T. Pierrehumbert, 2004) or annual mean surface temperatures (D. S. Abbot et al., 2013; Le Hir et al., 2010) approach 0°C. The former first appears in the subtropical regions while the latter appears in the equatorial region. This criterion is quite crude because melt ponds start to form on ice whenever the instant surface temperature is near 0°C (Polashenski et al., 2012), that is, at monthly mean surface temperatures much lower than 0°C since there will be strong diurnal and daily temperature fluctuations. Melt ponds have two effects on snowball Earth climate. The first is that it reduces the surface albedo and provides a positive feedback to the warming induced by increasing CO<sub>2</sub>. It may thus allow deglaciation to start at a lower CO<sub>2</sub> than when the melt pond is not considered. The second effect is that the melt ponds, if prevalent on the ice surface, may cause thick floating sea ice to fracture. This has been observed during the calving of ice shelf Larson B in Antarctic Peninsula (e.g., Banwell et al., 2013). Therefore, finding when and where extensive melt ponds appear on ice surface may tell us directly at what CO<sub>2</sub> concentration the deglaciation will start and whether the deglaciation starts from subtropical or equatorial region.

Melt ponds on ice can be considered in two distinctly different ways in climate models. The first is to simply parameterize its albedo effect by assuming a linear reduction of albedo with surface temperature. This is normal practice in sea-ice modeling in many climate models but they all differ in when the ice albedo starts to decrease and by how much (see Figure 1 of Hu et al., 2011). For example, in some models, the sea-ice albedo starts to decrease when the instant surface temperature is  $-10^{\circ}\text{C}$ , while others start at  $-1^{\circ}\text{C}$ , and some decrease the sea-ice albedo by as much as 0.25 while others may decrease by only 0.07 as temperature increases to 0°C. Moreover, such parameterization does not track the evolution of thickness of melt ponds and thus does not allow the melt ponds to persist through diurnal or seasonal cycles. A more sophisticated way of modeling the effect of melt ponds is to explicitly calculate their depth and their influence on albedo based on the depth. Our purpose herein is to develop such a scheme in the climate model and test how they will affect the deglaciation of a snowball Earth.

Melt ponds form on snow too, especially for thin snow on ice because melt water cannot percolate downward easily but accumulate on the surface; when undulations of snow thickness exist, as they normally do, melt ponds tend to form around snow dunes (Petrich et al., 2012; Webster et al., 2018). We do not intend to consider such detailed processes here but pay much attention to the effect of snow aging instead. The reason for this is that we found that the snow depth in a snowball Earth simulated by the climate model was always thick ( $\sim 1$  m water equivalent) except over a few narrow sublimation zone (e.g. Figure 4c) if the effect of snow

CLM3. Snow aging and its albedo effect are considered in CLM3 (Oleson et al., 2004), but not in the thermodynamic sea-ice module within CAM3 (Collins et al., 2004). Hu et al. (2011) prescribed thick sea ice over the ocean rather than treating sea ice as continental glaciers (e.g. D. S. Abbot et al., 2013), so they did have the effect of melt ponds (parameterized) on the albedo of both snow and ice but not the effect of snow aging. Without snow aging, their simulations gave very cold climate and melt ponds most likely did not take effect either. Moreover, their simulations were carried out for only a few tens of years, far from enough for initial deep snow (1 m water equivalent) on ice to sublimate and expose the ice below (Liu et al., 2020). Therefore, they found that the deglaciation of a snowball Earth could not be initiated even when the atmospheric CO<sub>2</sub> level ( $p\text{CO}_2$ ) was as high as 0.3 bar. We will show herein that the threshold  $p\text{CO}_2$  is much lower than 0.3 bar once the effect of snow aging is turned on and melt ponds are simulated in the same model. Moreover, we show that seasonal melt ponds develop first at subtropical regions but perennial and deep melt ponds appear first at the equator if melt ponds are simulated explicitly.

The rest of the paper is organized as follows. A brief description of the model used is provided in Section 2.1, the formulation for melt ponds on ice is described in Section 2.2, the experiments carried out in this study are summarized in Section 2.3. The results are presented in Section 3, and the uncertainties and implication of these results to snowball Earth deglaciation is discussed in Section 4. Finally, conclusions are reached in Section 5.

## 2. Model and Experimental Design

### 2.1. Climate Model and Snow Aging

The Community Atmosphere Model version 3 (CAM3) and Community Land Model version 3 (CLM3) used in this study were both developed by the National Center for Atmospheric Research. CAM3 solves the primitive equations in a generalized terrain-following vertical coordinate. The equations are solved with a spectral dynamic core with triangular truncation at wavenumber 31 (T31), which is equivalent to a horizontal spatial resolution of  $\sim 3.75^\circ \times 3.75^\circ$ . The model has 26 vertical levels from the surface to approximately 2 hPa (Collins et al., 2004). The module CLM3 deals with vegetation, wetland and lakes, glaciers, hydrological cycle on land, and thermodynamics of soil and snow (Oleson et al., 2004). Its horizontal resolution is the same as CAM3. The glaciers are prescribed in the module and thus cannot evolve. The albedo of glacier is 0.6 and 0.4 for the visible and near infrared wavebands, respectively, independent of the solar zenith angle. This albedo is typical for glacial ice (Paterson, 1994), and is similar to the sea-ice albedo used in Hu et al. (2011). For all simulations herein, sea ice is considered as glacier since it is very thick and moves slowly (generally smaller than 1 km/yr) like glaciers (Ashkenazy et al., 2014; J. C. J. G. R. L. Goodman, 2006; J. C. Goodman & Pierrehumbert, 2003; Tziperman et al., 2012).

The albedo of snow-covered ground is dependent on the thickness of snow and the solar zenith angle, and is distinguished for direct and diffuse beam radiation (Oleson et al., 2004). Here we only describe how snow age is determined and how it affects snow albedo in CLM3. Newly fallen snow has an age of zero, and its non-dimensional age increases with time as:

$$\tau_{\text{sno}}(t + \Delta t) = (1 - 0.1\Delta W_{\text{sno}}) [\tau_{\text{sno}}(t) + (r_v(T) + r_d)r_0\Delta t] \quad (1)$$

where  $r_0$  is  $1 \times 10^{-6} \text{ s}^{-1}$ ,  $\Delta t$  is the model time step,  $r_v$  takes into account of the effect of grain growth due to vapor diffusion and is dependent on snow temperature,  $r_d$  considers the effect of dirt, and  $\Delta W_{\text{sno}}$  is the change in mass of snow ( $\text{kg m}^{-2}$ ) relative to the last time step. The terms in the first bracket on the RHS means that if  $10 \text{ kg m}^{-2}$  (0.01 m water equivalent) of new snow falls on the surface of unit area ( $1 \text{ m}^2$ ), the snow age is restored to 0. The detailed form of  $r_v$  is not laid out here since we have no good reason to change it herein but its variation with temperature is shown in Figure 1a. The value of  $r_d$  is taken to be a constant, 0.3, by default in the model. However, since the amount of dust is uncertain during a snowball Earth, a few sensitivity tests will be carried out to test its influence on the snowball Earth climate. In these tests,  $r_d$  is reduced to 0.2, 0.1, and 0.03, respectively, and its influence on snow age is shown in Figure 1b. The non-dimensional snow age is reduced by  $\sim 14\%$  when  $r_d$  is reduced from 0.3 to 0.03. This change seems to be small but have significant influence on the simulated surface temperature in a snowball Earth.

Snow albedo decreases with the non-dimensional snow age according to

$$\alpha_{\text{sno},\Lambda} = \left[ 1 - C_\Lambda \left( 1 - \frac{1}{1 + \tau_{\text{sno}}} \right) \right] \alpha_{\text{sno},\Lambda,0} \quad (2)$$

where the albedo of new snow  $\alpha_{\text{sno},\Lambda,0}$  is 0.95 and 0.65 for the visible and near infrared wavebands and the empirical constant  $C_\Lambda$  is 0.2 and 0.5 for the two wavebands, respectively. The albedo of oldest snow is then 0.76 and 0.325 for the two wavebands, respectively (Figure 1c). The full spectrum average (with a partition of radiative flux between the visible and near-infrared wavebands being 53% vs. 47%) is thus 0.56, still higher than that for the glacier. In order to prevent melting of ice sheets over present-day Greenland and Antarctica, snow age has been hard coded to 0 in CLM3 whenever snow depth is greater than 800 mm. Such constraint is removed herein because we think that it will greatly overestimate the albedo of snow especially when precipitation rate is very low such as in a snowball Earth. Note that snow redistribution by wind is not considered in CLM3, what effect this might have on the simulated climate is thus unclear.

## 2.2. Melt Pond Formulation

Deglaciation of a snowball Earth must start with formation of melt ponds on the surface of thick sea-ice sheet. This process is not considered for the glaciers in CLM3, so we have to implement one by ourselves. In reality, melt ponds may consist of multiple layers of water and ice interleaved with each other due to seasonal, daily or diurnal melting and freezing (Hunke et al., 2013). Here we simplify the process by considering only three possible stages of the melt ponds: no melt pond, melt pond without and with one layer of ice lid (Figure 2). That is, we do not consider the formation of melt pond on ice lid and new layer of ice lid on this second layer of melt pond.

The vertical temperature profiles in the ice, melt pond and ice lid are also simplified (Figure 2). Right before melt ponds start to form, e.g., near noon of a certain day in summer, the temperature of near surface ice is assumed to be constant and at freezing point ( $T_f \equiv 0^\circ\text{C}$ ) of pure water (Stage I in Figure 2). This assumption is not bad since the heat of fusion of water is more than 80 times the heat required to raise the temperature of the same amount of ice by  $1^\circ\text{C}$ . After melt pond forms, the temperature profile is assumed to be linearly increasing from  $T_f$  at the bottom to the large scale (i.e., model-grid scale) ground surface temperature  $T_g$  calculated by the model. Such assumption is probably not so valid when the water temperature is below  $4^\circ\text{C}$  as pure water is densest at  $4^\circ\text{C}$ ; vertical convection will tend to reduce the temperature gradient so that the temperature profile may look more like the dotted curve in Stage II of Figure 2 (Bogorodsky et al., 2006; Roeckner et al., 2012; Scharien et al., 2014). This temperature profile is mainly used to calculate how much energy is being transferred to the bottom of pond and melting ice there. When the surface cools at night, an ice lid may form at the top of melt pond. In this stage, the temperature of water becomes  $T_f$  and the temper-

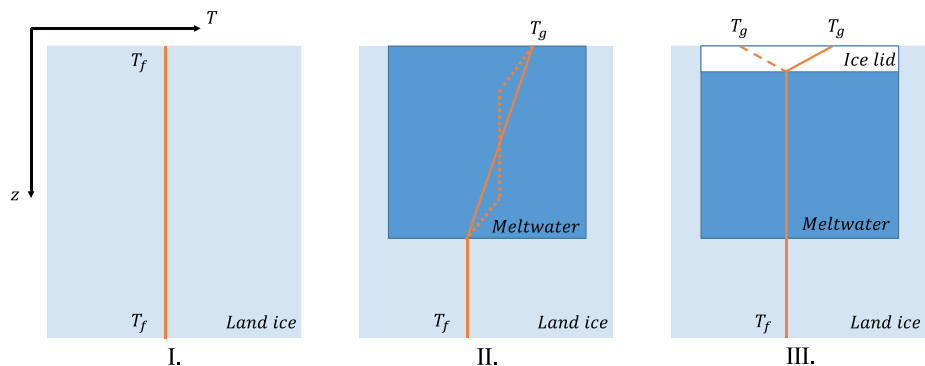


**Figure 2.** Melt ponds at different stages. The orange lines represent the vertical temperature profiles assumed in our melt pond formulation.  $T_f$  is the freezing temperature of pure ice, and  $T_g$  is the temperature at ground surface. The dotted line in stage II represents possible temperature profile when  $T_g$  is around  $4^\circ\text{C}$ .

ature within the lid is assumed to increase or decrease linearly from  $T_f$  at the bottom to surface temperature  $T_g$  at the top. This latter assumption of linearity is also a simplification of the reality because the interior temperature of the ice may not respond to surface temperature quickly, and it could be higher than the surface temperature due to penetration of sunlight into the ice interior.

The change of ice lid and pond water is governed by the Stefan condition at the phase boundaries (Hunke et al., 2013)

$$\rho_w L \frac{\partial h_w}{\partial t} \approx -k_w \frac{\partial T_w}{\partial z} \quad (3)$$

$$\rho_i L \frac{\partial h_l}{\partial t} \approx k_i \frac{\partial T_l}{\partial z} \quad (4)$$

where  $L$  is the latent heat of fusion of pure ice per unit volume,  $\rho_w$  and  $\rho_i$  are densities of ice and water,  $h_w$  and  $h_l$  are thicknesses of the pond water and ice lid,  $k_w$  and  $k_i$  are thermal conductivities of the melt-water and ice lid, and  $T_w$  and  $T_l$  are temperatures near the phase boundary of pond water and ice lid, respectively.

Because linear temperature profile has been assumed for the whole pond water, the magnitude of right-hand side (RHS) of Equation 3 may be either underestimated or overestimated. When pond water is thin, ice can melt by absorbing sunlight directly; when pond water is a few tens of centimeter thick, the temperature gradient may be strengthened near the bottom as shown in Figure 2 (middle); when pond water is a few meters thick, the temperature gradient may be strengthened again near the bottom because the temperature of water near the surface is well mixed beneath which a sharp thermocline forms as often observed in lakes (Axenrot et al., 2009; Schwarz et al., 2016). For these situations that are of the greatest relevance herein, the temperature gradient in the RHS of Equation 3 is underestimated. Only when pond water is very thick ( $>> 10$  m), the temperature gradient may be overestimated because water temperature tends be near constant below the thermocline in lakes (e.g. Stepanenko et al., 2010). Influence of the uncertainty in the temperature gradient of Equation 3 on the melt ponds and snowball Earth climate is tested in Section 4.1.

The magnitude of right-hand side (RHS) of Equation 4 is likely always overestimated; when ice lid is thin, sunlight can penetrate through the lid and increase its bottom temperature, while when it is thick, interior temperature of the lid responds slowly to the surface temperature and creates a relatively small temperature gradient near the bottom. Therefore, both Equations 3 and 4 are expected to underestimate the growth of pond water when the depth of water is not very thick (e.g.  $<10$  m). Note that ice lid has two phase boundaries. When surface temperature is high enough, melting always starts at the surface of the ice lid and melt water produced is assumed to leak into the melt pond beneath immediately. Nothing happens at the bottom of the lid. Also, no melting will start at the bottom of melt pond until the lid is completely melt away.

The ice surface is initialized to Stage I at the beginning of a run. Stage II starts to appear when the grid-scale surface temperature is greater than 0°C. When temperature decreases to below 0°C, Stage II will transform to Stage III but not necessarily all the way to Stage I before temperature starts to rise again. The thicknesses of pond water and ice lid are tracked at every time step of the model run. Unlike sea ice of present day, which is thin and pond water may leak into the ocean beneath easily through leads (Eicken et al., 2002; Richter-Menge et al., 2001), the sea ice is so thick during a snowball Earth that we do not need to worry about the loss of pond water on short timescales, e.g. months. When melt water is deep enough, its weight might cause the ice sheet to break and fracture, then melt water will drain into the ocean beneath ice. This process is not explicitly modeled here but its effect is discussed by limiting the melt-water depth to 0.5 m and 0.2 m in two experiments.

The surface albedo of infinitely thick ice is affected by the presence of pond water (Taylor & Feltham, 2004),

$$\alpha_p = R_0 + \frac{(1 - R_0)^2 s_{ice} e^{-(\tau+2\kappa)h_w}}{1 - R_0 s_{ice} e^{-(\tau+2\kappa)h_w}}, \quad s_{ice} = \frac{\alpha_i - R_0}{1 - 2R_0 + \alpha_i R_0} \quad (5)$$

where  $\alpha_i$  is the albedo of infinitely thick ice (the albedo of glacier) and  $\alpha_p$  is the albedo when there is melt pond of  $h_w$  thick.  $R_0 = 0.05$  is the Fresnel reflection coefficient of water,  $\tau = 3.55$  is the fitting parameter,  $\kappa = 0.025 \text{ m}^{-1}$  is the extinction coefficient of water. When ice lid of  $h_l$  is present, the surface albedo becomes (Briegleb et al., 2004)

$$\alpha_e = f_h \cdot \alpha_i + (1 - f_h) \cdot \alpha_p, f_h = \min\left(\frac{\arctan(c_{fh} \cdot h_l)}{\arctan(c_{fh} \cdot h_c)}, 1.0\right) \quad (6)$$

where  $c_{fh} = 4$ ,  $h_c = 0.5 \text{ m}$  are empirical parameters, arctan is the inverse tangent function. When the thickness of ice lid is greater than 0.5 m, the effective surface albedo is equal to the albedo of glacier.

To get the surface albedo of a grid cell of the climate model, the areal fraction of melt pond within the grid cell is needed. We assume that the temperature at any point (e.g., with an area of  $1 \text{ m}^2$ ) is random due to turbulence in the atmosphere and fluctuates around the grid cell temperature according to a normal distribution, with a standard deviation  $\sigma = 1^\circ\text{C}$ . Then the fraction of grid cell that has temperature greater than  $T_f$  is

$$C = 1 - \Phi\left(\frac{T_f - T_g}{\sigma}\right) \quad (7)$$

where  $\Phi$  is cumulative distribution function of the standard normal distribution (Ross, 2010). Note that this fraction is greater than zero even when  $T_g$  is  $20^\circ\text{C}$  below  $T_f$ , but is negligible. We calculate the formation of melt pond only when  $T_g$  range from  $T_f - 2\sigma$  and  $T_f + 2\sigma$ . The average temperature over this part of the grid cell is

$$\bar{T}_{gmelt} = T_g + \frac{\sigma}{C\sqrt{2\pi}} e^{-\frac{(T_f - T_g)^2}{2\sigma^2}} \quad (8)$$

This temperature is used to calculate the thickness of meltwater within each grid cell. The calculated thicknesses are then multiplied by factor C to get grid-mean thicknesses, which is used to calculate the grid-mean surface albedo. The value of  $\sigma$  is uncertain but  $1^\circ\text{C}$  should be an underestimate; without considering the air turbulence, the temperature difference between the southern and northern boundaries of a grid cell can be greater than  $1^\circ\text{C}$  even in the low-latitude region due to the coarse resolution of the model. Increasing of  $\sigma$  enhances formation of melt pond (see Section 4.1).

### 2.3. Experimental Design

In all experiments carried out herein, continents and oceans are not distinguished since both of them are covered by thick ice. The surface of the whole globe is treated as continental glacier, similar to the setup in D. S. Abbot et al. (2013). The surface topography is ignored, to be consistent with the model setup in Hu et al. (2011). The initial snow depth is uniformly 1 m water equivalent. Present-day orbital configuration of the Earth is assumed. The atmospheric concentrations of  $\text{CH}_4$ ,  $\text{N}_2\text{O}$  are all pre-industrial level. CFCs are set to zero. In all experiments carried out here, solar constant is 94% of present-day value and  $p\text{CO}_2$  is 0.1 bar.

Three sets of experiments are carried out. In the first set of five experiments, the climate impact of snow aging is tested. Effect of melt pond is not considered in this set of experiment. The first experiment (experiment Default) uses the default setting for snow aging calculation, i.e., snow age is fixed to 0 for snow deeper than 800 mm water equivalent, and the other four experiments (rd1 to rd4) removes the restriction. In these four experiments, the snow aging parameter  $r_d$  is set to 0.3, 0.2, 0.1, and 0.03, respectively. In the second set of three experiments, the influence of melt pond on climate of snowball Earth near deglaciation is tested. In two of the three experiments (IMP80 and IMP60), implicit melt pond is considered; surface albedo of ice decreases linearly with instant surface temperature to 80% and 60% of the original value when instant temperature becomes  $0^\circ\text{C}$  for the two experiments, respectively (Figure 3). In the third experiment (EMP\_rd1), melt ponds on ice are explicitly modeled using the formulation above. In all three experiments, the snow ag-

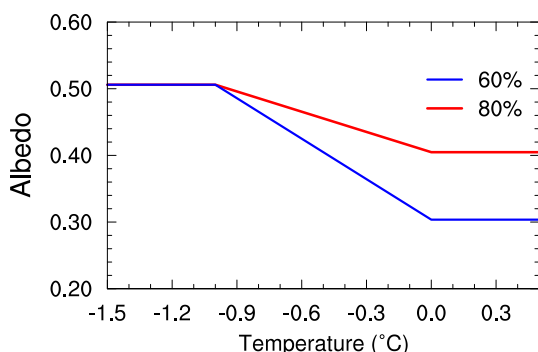


**Figure 3.** The linear dependence of surface albedo of ice on temperature in the implicit formulation of melt ponds.

ing parameter  $r_d$  is fixed to 0.3. The first four of the third set of six experiments (EMP\_rd1, ..., EMP\_rd4) is the same as the last four experiments of the first set except that here the explicit simulation of melt ponds is implemented. The other two experiments of the third set are carried out to test the possible influence of active melt-water drainage by limiting the maximum water depth to 0.5 m (EMP\_rd1\_L5) and 0.2 m (EMP\_rd1\_L2), respectively. The second and third sets share one experiment, EMP\_rd1. All simulations are continued for at least 400 years, and the last 50 years are used for diagnosis of equilibrium climate state.

### 3. Results

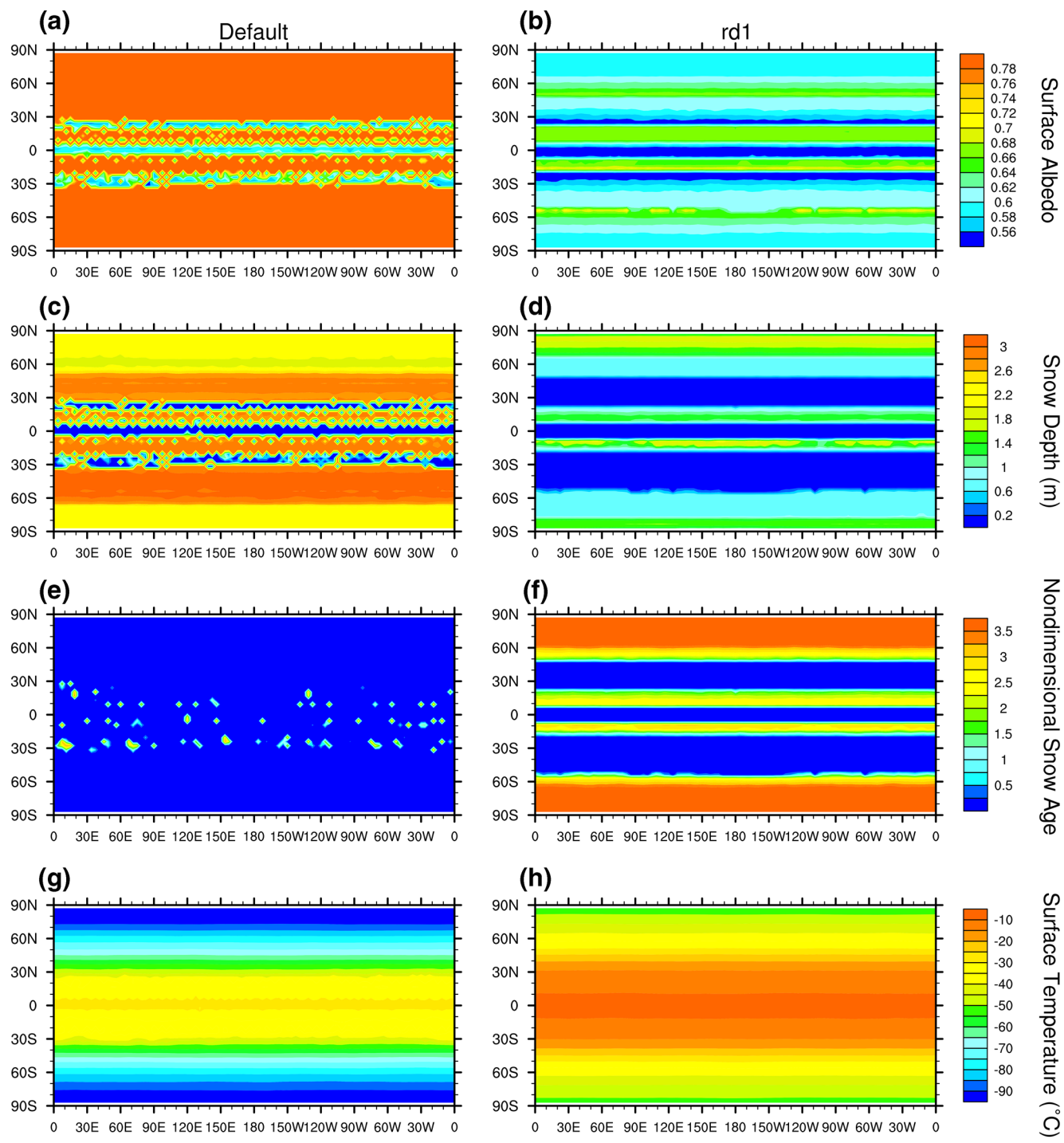
#### 3.1. Influence of Snow Aging on the Snowball Earth Climate

In the default CLM3, snow age is forced to be zero when water equivalent snow depth is greater than 800 mm and initial snow depth on glaciers is 1,000 mm. In this case, the surface albedo of the whole globe is high for a snowball Earth unless the climate warms up significantly so that snow depth decreases to below 800 mm. This does not happen even when  $p\text{CO}_2$  is 0.1 bar except over three narrow belts around the equator and in subtropical regions where sublimation is strong (Figures 4a and 4c). If the 800 mm restriction is removed, global snow age increases (Figure 4f) and surface albedo decreases significantly (Figure 4b). This causes the surface temperature to increase dramatically (compare Figures 4h–4g) and snow coverage to decrease (Figure 4d). At equilibrium, the global mean surface temperature is  $-19.9^\circ\text{C}$ ,  $31.1^\circ\text{C}$  higher than in experiment Default. To be consistent with the melt pond formulation in Section 2.2, all surface temperature shown herein mean ground surface temperature.

There is significant seasonal variability in precipitation and snow age due to seasonal change in solar insolation (Figure 5). In general, there is little precipitation during winter and spring in polar regions (Figure 5c), allowing snow age to grow to a maximum in May. This helps reduce the surface albedo there in the late spring and early summer (Figure 4b). As latitude decreases, snow precipitation starts at earlier and earlier time, giving less time for snow age to grow and surface albedo to decrease (see the region between  $\sim 45^\circ$  and  $65^\circ$  latitude in Figure 4b). Within the subtropical region ( $\sim 25^\circ$ – $45^\circ$  latitude), snow age is always near zero due to either continuous refreshening of the surface by snow or complete absence of surface snow (Figures 5c–5e). Due to the absence of snow over approximately a third of the year owing to very strong summer insolation (Figures 5a and 5b), the annual mean surface albedo within this region is low (Figure 4b). The situation is similar in the equatorial region where snow age is also zero but surface albedo is low due to little snow accumulation, except that the reason here is that the solar insolation is relatively high all through the year (Figures 5a and 5b).

The hydrological cycle is greatly enhanced (Figure 6) due to the change of surface temperature (Figure 4b); both precipitation (Figure 6b) and evaporation rates (Figure 6c) are increased by about a factor of five in the tropical region. Some of the increased precipitation is in the form of rain in the mid-latitude region (as can be inferred from the fatter red curve in Figure 6b compared to that in Figure 6a). This rain happens primarily during summer (not shown). This enhanced hydrological cycle does increase the net snow accumulation in the mid to high-latitude regions and the outer tropical region ( $\sim 10^\circ$ – $20^\circ$  latitude, around the intertropical convergence zone [ITCZ]), but it also increases net evaporation in the equatorial region and the subtropical region (compare the red curve to black curve in Figure 6d).

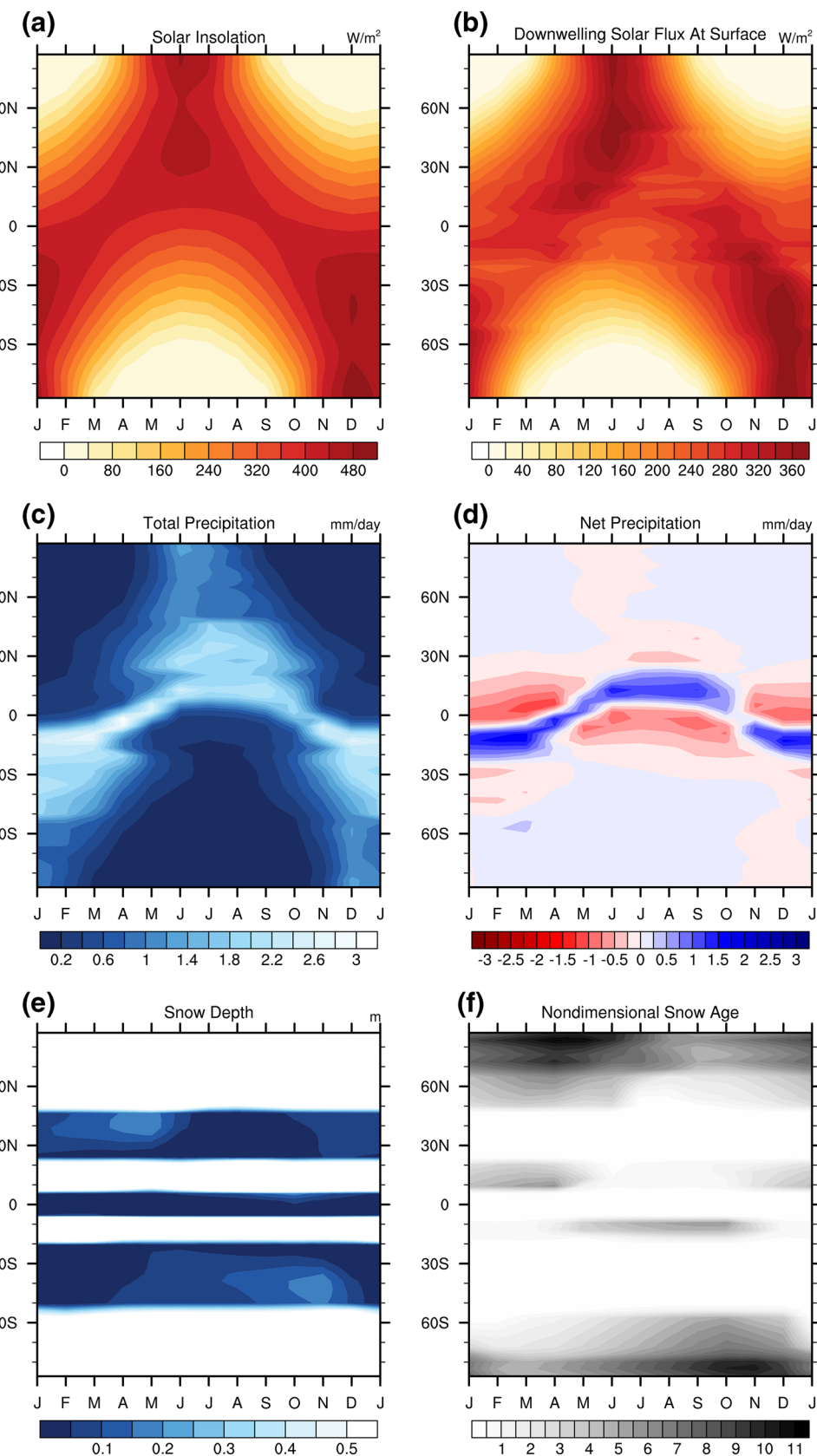
The global mean surface temperature is almost the same when  $r_d$  is decreased from 0.3 to 0.2, and lowered by  $1.0^\circ\text{C}$  and  $1.7^\circ\text{C}$  when  $r_d$  is further decreased to 0.1 and 0.03, respectively (Table 1). Although temperature change is small, the time it takes for the climate to reach equilibrium increases significantly when  $r_d$  is reduced (Figure 7). The annual mean temperature around the equator ( $6^\circ\text{S}$ – $6^\circ\text{N}$ ) is  $-7.7^\circ\text{C}$  and the highest monthly temperature is  $-3^\circ\text{C}$  when  $r_d = 0.3$ , both below the melting temperature of ice. The highest monthly temperature is found over the subtropical regions and is higher than  $0^\circ\text{C}$  (Figure 8). Clearly, these high temperatures will initiate seasonal melting. Whether that will initiate deglaciation of snowball Earth is hard to judge without considering the effect of melt ponds.



**Figure 4.** Annual-mean surface albedo (a), (b), snow depth (c), (d), nondimensional snow age (e), (f) and surface temperature (g), (h) at equilibrium state. Panels on the left and right are for Experiments Default and rd1, respectively. Note that the deep blue in (e) indicates thick (>800 mm water equivalent) snow while in (f) it indicates thin (a few 10 s of mm) new snow.

### 3.2. Influence of Melt Ponds on Snowball Earth Climate

Melt ponds indeed have a strong effect on the snowball Earth climate whether they are represented implicitly or explicitly in the model (Figure 9). The implicit melt ponds start to take effect quickly, within a few years if the more aggressive parameter is used (experiment IMP60; Figure 9d). In this case, the annual mean



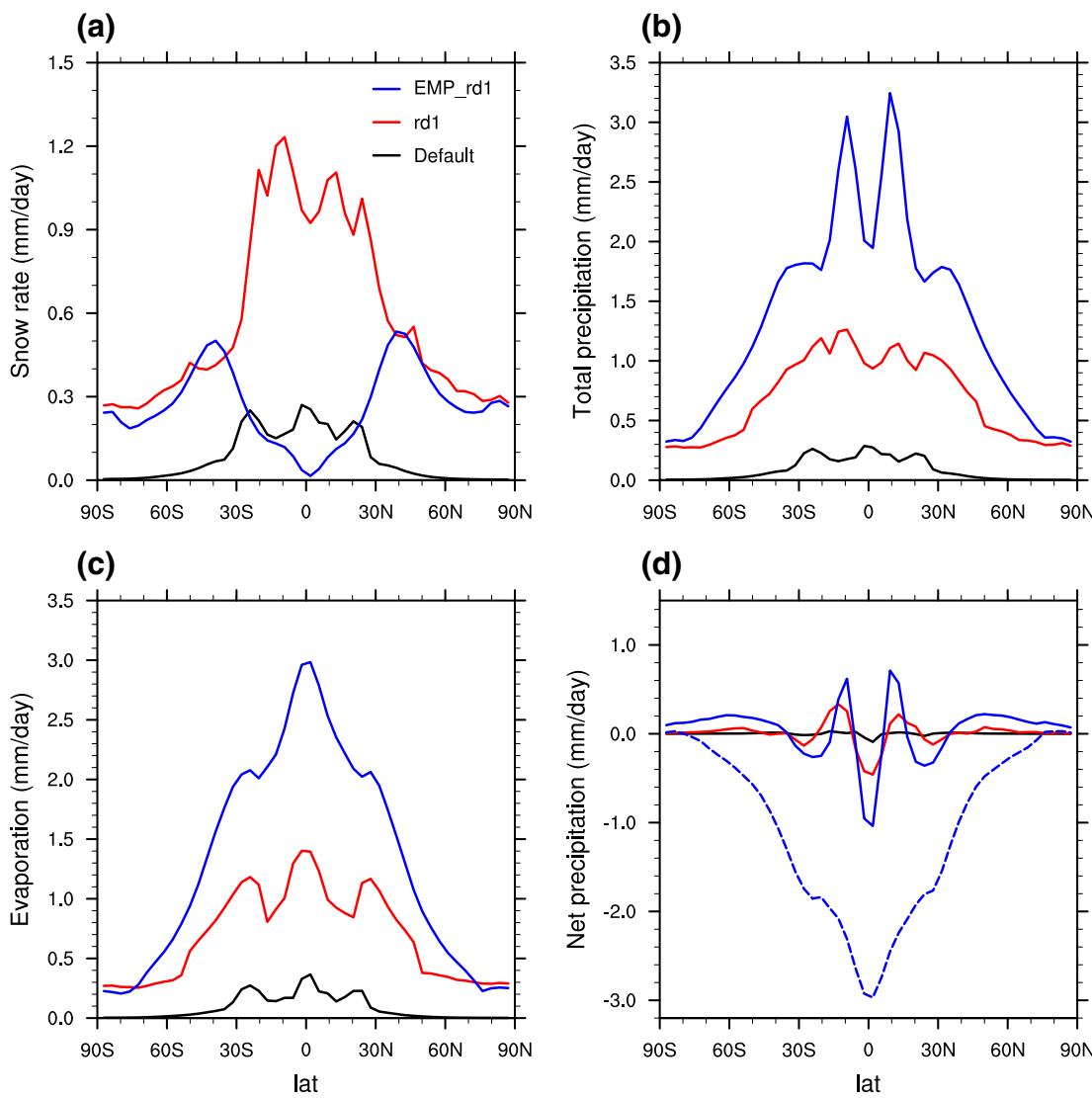


**Figure 6.** Zonally averaged annual-mean (a) snow rate, (b) total precipitation, (c) evaporation, and (d) net precipitation obtained in experiments Default, rd1, and EMP\_rd1. In (d), the dashed line is net accumulation rate (snow rate-evaporation), assuming that all rain drain into the oceans. Note that the y-axis limits are different in different panels.

surface temperature around the equator rises from about  $-13.0^{\circ}\text{C}$  to the equilibrium temperature of  $2.7^{\circ}\text{C}$  within 20 years, while it takes 50 years to rise to only  $-7.8^{\circ}\text{C}$  when melt ponds are not considered (Figure 9a). When the less aggressive parameter is used (experiment IMP80), temperature rises more slowly and the equilibrium temperature is  $-0.5^{\circ}\text{C}$  (Figure 9c). The global mean surface temperature is approximately  $13^{\circ}\text{C}$  lower than that around the equatorial mean in all these three cases (Figure 9).

When the melt ponds are simulated explicitly (experiment EMP; Figure 9b), the time it takes for temperature to reach equilibrium is longer than that when implicit melt ponds are used. This is probably not surprising because the melt ponds in this case take time to develop. The final equatorial temperature is  $6.1^{\circ}\text{C}$ , much higher than those for experiments IMP80 and IMP60. This is not surprising either because explicit melt ponds can grow to large depth (black dashed curve in Figure 9b), and the surface albedo will be near

**Figure 5.** Seasonal variation of (a) solar insolation at top of atmosphere, (b) downwelling solar radiation at the surface, (c) precipitation rate, (d) net precipitation rate, (e) snow depth, and (f) non-dimensional snow age. The units are  $\text{W m}^{-2}$ ,  $\text{mm/day}$  and  $\text{m}$  for insolation, precipitation rate, and snow depth. The results are from a simulation without melt ponds (Experiment rd1).

**Table 1**  
*Summary of Experiments and Main Results*

Experiment	Snow aging parameter $r_d$	6°S – 6°N Temperature (°C)	Global temperature (°C)	Start year of deglaciation	Surface albedo
Default	0.3 <sup>a</sup>	-29.1	-51.0	–	0.74
rd1	0.3	-7.7	-19.9	–	0.61
rd2	0.2	-7.9	-20.1	–	0.61
rd3	0.1	-9.1	-21.1	–	0.62
rd4	0.03	-9.7	-21.8	–	0.62
IMP80	0.3	-0.4	-13.7	–	0.53
IMP60	0.3	2.7	-9.9	15	0.46
EMP_rd1	0.3	6.1	-6.9	40	0.38
EMP_rd2	0.2	6.1	-7.0	65	0.39
EMP_rd3	0.1	-7.7	-18.3	–	0.59
EMP_rd4	0.03	-7.8	-18.6	–	0.59
EMP_rd1_L2	0.3	1.9	-11.4	41	0.49
EMP_rd1_L5	0.3	5.1	-7.8	38	0.41

<sup>a</sup>Snow age is fixed to 0 for snow that is deeper than 800 mm water equivalent.

that of oceans when the pond depth is greater than 1 m. Once the pond is deeper than 1 m, further growth in depth will not have any additional climate effect.

We could have varied the parameter of the implicit melt pond so that its surface albedo continuously decreases when instant temperature is greater than 0.0°C, for example, to 0.1 when temperature is 5°C. However, it will be very unrealistic because low albedo (equivalent to deep melt pond) will appear suddenly at noon even though the annual mean temperature is below -20°C and the monthly mean temperature of the warmest month is -7°C (not shown). Our explicit melt-pond modeling shows that deep ponds (>10 cm) appear only when monthly mean surface temperature is greater than  $T_f$  (Figure 10).

An example of seasonal evolution of melt pond in the subtropical region (16.7°N) at model year 40–41 is shown in Figure 10. Note that at this time for this specific case, the depth of melt pond is still evolving and has a net increase each year (Figure 10b), so is the temperature (Figure 10a). Melt water appears in all months shown in the figure, but is very shallow and appears only in certain hours of a day during the cold months. In the first February of the figure, monthly mean temperature is -10°C, but the maximum instant temperature can be as high as -0.05°C, making formation of melt ponds possible. The mean depth of melt ponds for this month is only 0.2 mm. This depth increases rapidly

to 9 cm in May, and increases to a maximum of 60 cm in early December (Figure 10b). Ice lid starts to develop near the end of December but its thickness is negligible. It grows to a maximum of ~60 cm in the second April and then starts to decrease. At this time, there is still melt water beneath the ice lid but the lid is thick enough so that the surface albedo is the same as that of glaciers (Figure 10c). Near the end of the second June, ice lid disappears and the thickness of pond water recovers to its maximum during the last year. The pond water continues to grow from the second July to early December, becomes deeper than in the last year (Figure 10b). See the video in supporting information for the complete evolution of the surface melt ponds.

When explicit melt ponds are considered (experiment EMP\_rd1), the hydrological cycle is enhanced further compared to case where only snow aging is considered (experiment rd1); the maximum annual-mean evap-

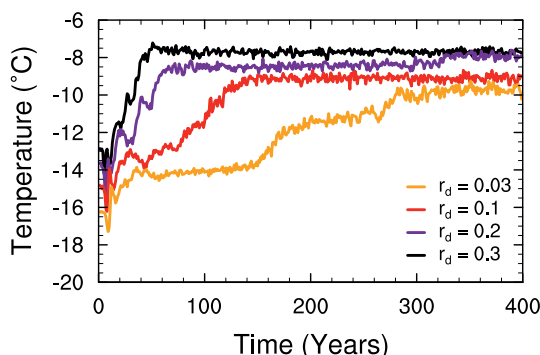


**Figure 7.** Time series of annual mean equatorial (6°S–6°N) surface temperature for Experiments rd1 to rd4.

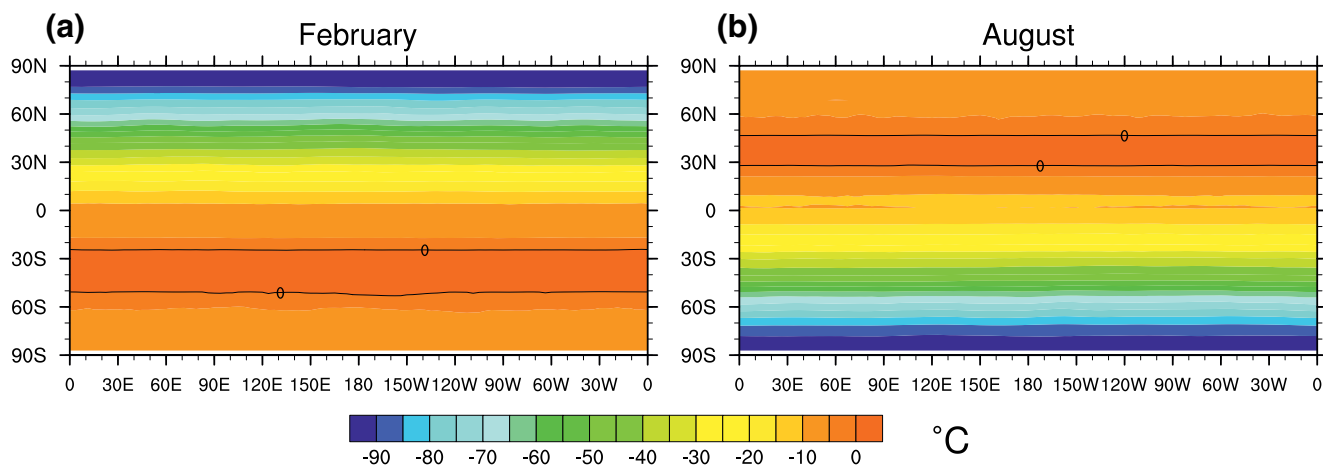


**Figure 8.** Monthly mean surface temperature for February and August in Experiment rd1 at equilibrium.

oration (at equator) increases from  $\sim 1.4$  mm/day to  $\sim 3.0$  mm/day (Figure 6c), and the maximum annual-mean precipitation (at ITCZ) increases from  $\sim 1.2$  mm/day to  $\sim 3.2$  mm/day (Figure 6b). However, the snow rate decreases dramatically in the tropical region and changes little in other regions (Figure 6a). This means that most of precipitation is in the form of rain. In the tropical region, the melt water is being evaporated continuously but is then replenished as rain.

If the difference in snow rate and evaporation (the former minus the latter) is used as the surface mass balance of the ice sheet, it is highly negative (blue dashed curve in Figure 6d). This negative surface balance will reduce ice thickness quickly in the tropical region ( $\sim 0.8$  m/yr) if meltwater and rain are draining into the oceans through cracks on ice at a fast rate but not fast enough to expose the ice surface and raise the surface albedo. This is discussed further in Section 4.5.

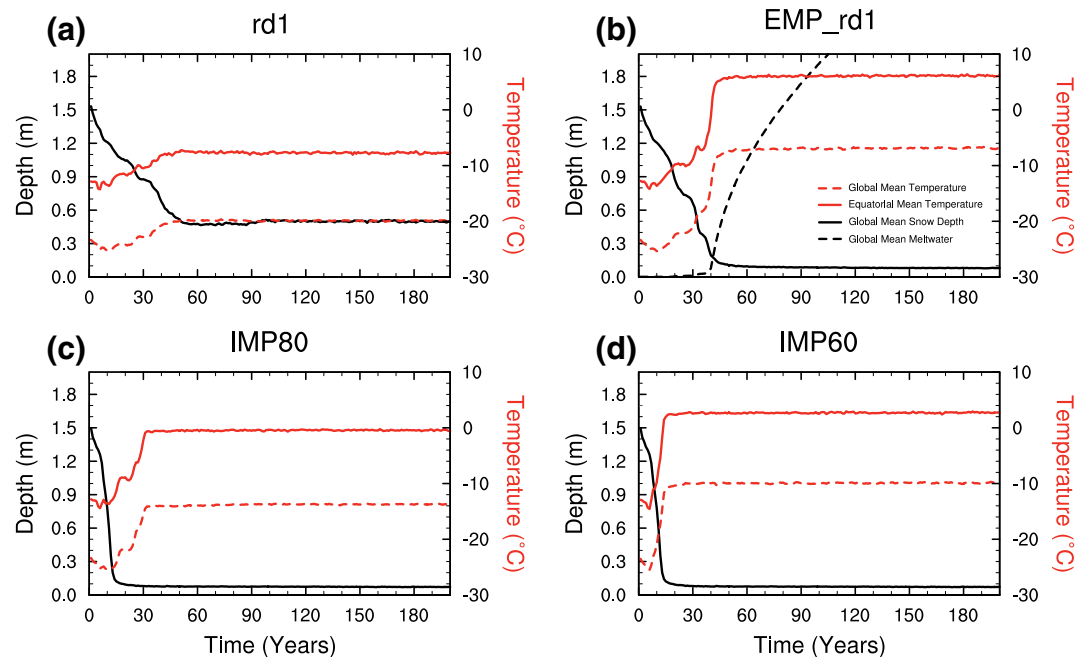


**Figure 9.** Annual-mean equatorial ( $6^{\circ}\text{S}$ – $6^{\circ}\text{N}$ ) mean surface temperature (red solid curve), global mean surface temperature (red dash curve), and global mean snow depth (black solid curve) for the (a) Default, (b) EMP\_rd1, (c) IMP80, and (d) IMP60. Black dashed curve in (b) represents global mean thickness of melt water.

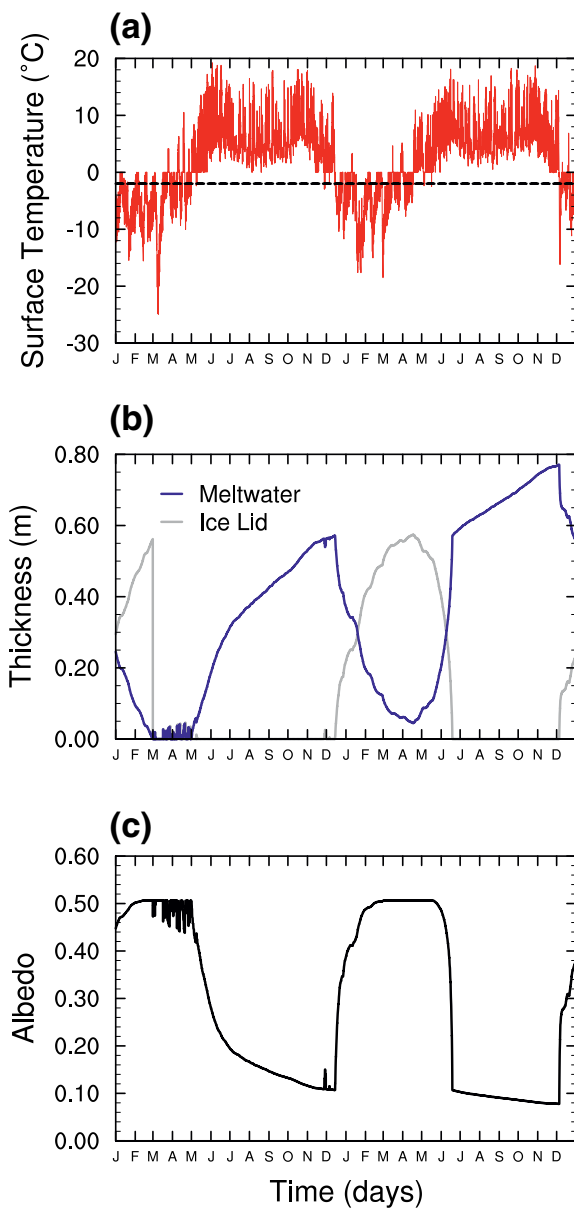


**Figure 10.** Time series of daily (a) surface temperature, (b) thickness of meltwater and ice lid, and (c) albedo from model year 40–41 at a point located at  $(180^{\circ}\text{E}, 16.7^{\circ}\text{N})$  in Experiment EMP\_rd1. The black dashed line in (a) indicates the temperature  $-2\sigma$  (where  $\sigma = 1^{\circ}\text{C}$ ) above which the formation of melt pond is possible.

#### 4.2. Availability of Dust

Results in Section 3.3 indicate that the dust effect on snow aging cannot be much weaker than that in present day in order for the effect of melt ponds to kick in. Using a one-dimensional model, Abbot and Halevy (2010) estimated that dust could be abundant in the atmosphere due to weak hydrological cycle in a snowball Earth. In their estimate, dust sources were limited to unglaciated land. An additional source could be the dust locked in the thick sea ice during long snowball Earth period and transported to the net sublimation region of low latitude (Hoffman et al., 2017; D. Li & Pierrehumbert, 2011). Moreover, because snow precipitation rate is small during a snowball Earth, little dust may be needed to mix with surface snow in order for it to age. Therefore, we may expect that snow aging near the end of a snowball Earth event was

#### 3.3. Influence of Snow-Aging Parameter when Melt Ponds are Considered

In contrast to results in Section 3.1 (e.g. Figure 7), the snowball Earth climate is much more sensitive to the snow-aging parameter  $r_d$  when melt ponds are considered (Figure 11). Annual mean equatorial temperature is  $\sim 6.1^{\circ}\text{C}$  for both  $r_d = 0.3$  and 0.2, while it is only  $-7.7^{\circ}\text{C}$  when  $r_d = 0.1$  and 0.03 (Table 1). The latter is almost the same as the temperatures obtained when melt ponds are not considered (experiments rd3 and rd4, Table 1). This is a clear indication that the melt ponds are basically not forming when  $r_d$  is small. Therefore, existence of dust in the snowball Earth climate is very important to snow aging and its deglaciation.

### 4. Discussion

#### 4.1. Further Sensitivity Test of the Explicit Melt Pond Model

In Section 2.2, the surface temperature is assumed to fluctuate within a grid cell which has a size of  $3.75^{\circ} \times 3.75^{\circ}$ , and the standard deviation ( $\sigma$  in Equation 7) of the fluctuation is assumed to be  $1^{\circ}\text{C}$ . Although we have argued that  $1^{\circ}\text{C}$  is small compared to the temperature change between the southern and northern boundaries of the grid cell, it is helpful to test how sensitive the results are to the value of this parameter. The results are shown in Figure 12a. It can be seen that the equilibrium equatorial temperature is insensitive to the change of  $\sigma$  within the range  $0^{\circ}\text{C}$ – $2^{\circ}\text{C}$ . When  $\sigma$  is lowered to  $0.25^{\circ}\text{C}$ , development of melt ponds nearly halts and the equatorial temperature is similar to when melt ponds are not considered (experiment rd1; Table 1). These tests show that as long as  $\sigma$  is large enough so that some formation of melt ponds can trigger, the positive feedback between the climate and melt ponds will drive the climate to a warm state and further increasing  $\sigma$  is not useful. Therefore, moderate temperature fluctuation of  $\pm 1.5^{\circ}\text{C}$  ( $3\sigma$  where  $\sigma = 0.5^{\circ}\text{C}$ ) within a large grid cell is enough to trigger prevalent formation of melt ponds and snowball Earth deglaciation (see discussion below) when  $p\text{CO}_2$  is 0.1 bar.

In formulating the melt pond model, we also assumed that the temperature profile of pond water is linear (Figure 2). Since this temperature gradient of water determines the downward growth of pond water (Equation 3), it is necessary to test how sensitive the result is to this temperature gradient. The results show similar bifurcation behavior as those for the tests of  $\sigma$  (Figure 12), i.e. as long as the gradient is 0.75 times or larger than that implied by the linear temperature profile, melt ponds will develop significantly and deglaciation will start.

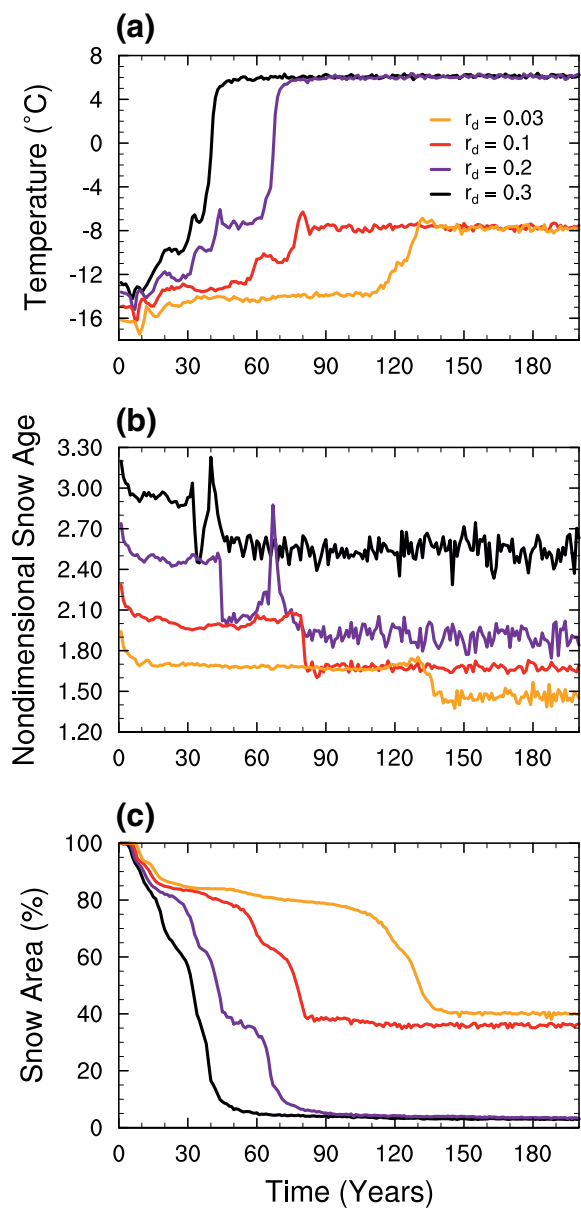


**Figure 11.** Time series of annual-mean of (a) equatorial ( $6^{\circ}\text{S}$ – $6^{\circ}\text{N}$ ) surface temperature, (b) global mean non-dimensional snow age, and (c) snow area (both averaged over area only where snow depth is greater than 0.3 m) for Experiments EMP\_rd1, to EMP\_rd4.

equatorward flow of melt water is non-negligible, it will only promote the earlier appearance of melt water in the tropical region.

Last of all, the ice elevator will expose dust accumulated over millions of years to the ice surface over the subtropical regions. The effect of such dust is not considered in the present study. Since such dust lowers the surface albedo of subtropical regions just like what the melt ponds do in the mid-latitude regions, it may be expected that this dust would also induce the appearance of perennial melt ponds over the equatorial region, at an even lower  $\text{CO}_2$  level. It is also possible that the seasonal melt water in the subtropical region flushes the dust into the bottom of discrete lakes or into oceans through cracks on sea ice as will be discussed below in Section 4.5. In any case, the existence of such dust does not affect the deglaciation process

as effective in reducing snow albedo as in present day even if atmospheric dust loading might be lower.

#### 4.3. Possible Influence of Sea-Glacier Dynamics

The sea ice is hundreds of meters thick during a snowball Earth. It deforms under its own weight like a continental glacier, and has therefore been termed as “sea glacier” (Goodman & Pierrehumbert, 2003). The velocity of the glacier is only a few tens of meters per year in the polar region and increases to  $\sim$ 1–2 km/yr in the tropical region (Campbell et al., 2014; Goodman & Pierrehumbert, 2003; Goodman & Strom, 2013; Li & Pierrehumbert, 2011; Tziperman et al., 2012). Nevertheless, such velocity is critical in maintaining a very small meridional gradient in ice thickness (Pollard & Kasting, 2005) and thus surface slope. The difference in ice thickness between the equator (thinner) and poles (thicker) is smaller than 500 m (e.g. D. S. Abbot et al., 2013; Tziperman et al., 2012), meaning a difference in surface elevation of smaller than 50 m and a meridional surface slope of smaller than 0.5 m per 100 km. The movement of sea glacier is also very important in transporting meteoric ice formed at mid- to high-latitude regions (J. C. J. G. R. L. Goodman, 2006) and dust contained in the mid- to high-latitude ice toward the low-latitude regions (J. C. Goodman & Strom, 2013; D. Li & Pierrehumbert, 2011). In the subtropical regions and equatorial region where there is a net evaporation, the ice moves upwards (D. Li & Pierrehumbert, 2011) and the dust it contains will be exposed to the surface (the so-called ice elevator theory; R. Pierrehumbert et al., 2011). These dynamics of sea glaciers are not considered in the present model, and their possible effect is discussed below.

First of all, the velocity of sea glacier is at least 3 orders of magnitude smaller than typical winds (1 m/s or 30,000 km/yr), oceanic and sea-ice currents (0.1 m/s or 3,000 km/yr). Thus, the movement of sea glacier should not have any significant influence on the momentum budget of the atmosphere and the simulated climate dynamics. Also, it takes thousands of years for sea glacier to move from mid-latitude where melt ponds first appear to the deep tropics where perennial melt ponds appear, while it takes only a few years for tropical melt ponds to evolve from non-existent to extensive and deep (e.g.  $>0.2$  m; Figure 9b). Therefore, the transport of melt water by sea glacier toward the equator is negligible.

Second of all, the melt water produced in the mid-latitude region may flow toward the equator due to the lower surface elevation there. Such flow is expected to be insignificant given the mild slope of ice surface. The melt water will more likely gather toward local depressions that appear randomly due to spatial variations in surface temperature (e.g. Figure 13) due to atmospheric turbulence, forming discrete lakes. Even if the

equatorward flow of melt water is non-negligible, it will only promote the earlier appearance of melt water in the tropical region.

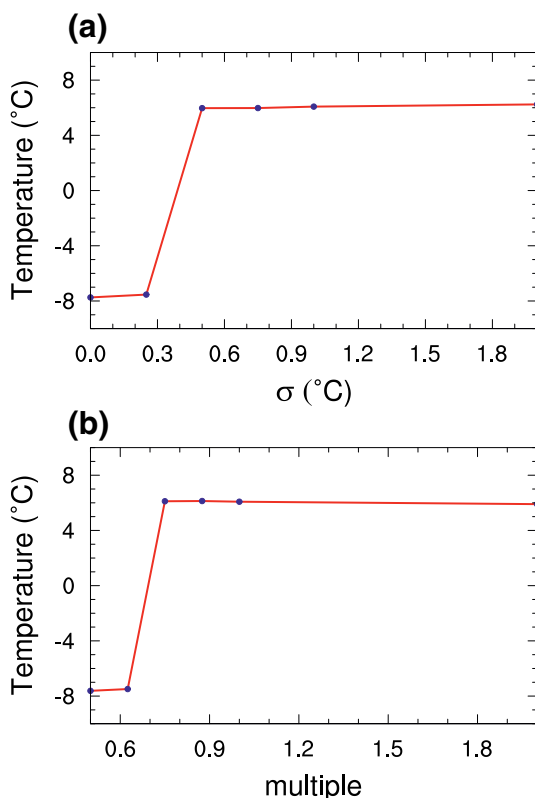


**Figure 12.** Sensitivity of equilibrium annual mean equatorial ( $6^{\circ}\text{S}$ – $6^{\circ}\text{N}$ ) surface temperature to (a)  $\sigma$  in Equation (7) and (b) temperature gradient in Equation (3). The experimental setup is the same as EMP\_rd1.

discussed in this study except that it allows the deglaciation to occur at a lower  $\text{CO}_2$  level.

#### 4.4. Difference in Results Between Implicit and Explicit Melt Ponds

In the implicit melt pond formulation, surface temperature can be used as a surrogate for appearance of melt ponds. Taking the experiment IMP80 as an example, narrow belt of melt water appears seasonally between  $23^{\circ}\text{N}$ – $33^{\circ}\text{N}$  and  $22^{\circ}\text{S}$ – $60^{\circ}\text{S}$  (Figures 13a and 13b) at model year 25. These belts of melt water expands substantially at equilibrium and the maximum monthly mean temperature can be as high as  $8^{\circ}\text{C}$  (Figures 13c and 13d). At such high monthly temperature, it may be expected that deep melt ponds form and sustain through the year. However, they always disappear completely during winter under such formulation. Moreover, it is suspicious that subtropical temperature can reach this high (compared to the temperature at equator); the too easy formation of melt ponds and strong positive feedback between melt-pond albedo and temperature may have induced this surprisingly high monthly temperature.

In this formulation, melt-pond albedo does not decrease once the surface temperature is higher than  $0^{\circ}\text{C}$  (Figure 3). Otherwise, the temperature in these two regions can be even higher and it might give you the illusion that deglaciation of snowball Earth will start from these regions. There is no permanent melt ponds appearing at equator, as can be inferred from Figures 13c and 13d. Therefore, it is hard to know where the deglaciation will start even when a formulation for implicit melt pond is included in the model. If a more aggressive formulation is used, e.g. experiment IMP60, permanent melt pond appears near the equator (not shown), but the maximum monthly temperature in the subtropical regions can reach  $12^{\circ}\text{C}$ , which again suggest heavy melting and probable deglaciation there.

Inclusion of explicit formulation of melt ponds in the model removes the ambiguity above. Although melt ponds first appear seasonally in the mid latitude region during the run (Figures 14a and 14b), permanent deep melt ponds appear only within a wide belt ( $\pm 20^{\circ}$  latitude) around the equator at equilibrium (Figures 14c and 14d). The results also tell us that the maximum monthly surface temperature at mid latitude can reach  $\sim 15^{\circ}\text{C}$  (Figure 15c) without forming permanent melt ponds, because the minimum monthly temperature at the same location can be as low as  $-40^{\circ}\text{C}$  (Figure 15).

The depth of water at equator reaches 10 m at model year 200 and continues to grow with time (not shown). It demonstrates that at the end of a snowball Earth, large swamps of water appear over more than half of the globe at all seasons, but deep perennial water accumulates only at the equator. Eventually, such deep water should become thick enough to break the ice sheet and start the deglaciation, see more discussion below.

#### 4.5. Deglaciation of a Snowball Earth

The dynamics of sea glacier over oceans during a snowball Earth is similar to the ice shelves around Antarctica. The largest difference between them is that the ice movement in the former is restricted in all directions since there is no open ocean, while the ice shelves in the latter can move freely toward the ocean in some direction. Nevertheless, the disintegration of the ice shelves may provide some clue for how the snowball Earth starts to deglaciate. Many of the disintegration events around Antarctica had been observed and the mechanisms studied (T. A. Scambos et al., 2000; T. Scambos et al., 2009). Among these events, the most significant one may be the disintegration of the Larsen B ice shelf, approximately  $3,250\text{ km}^2$  collapsed in just a few days in March 2002 (Shepherd et al., 2003).

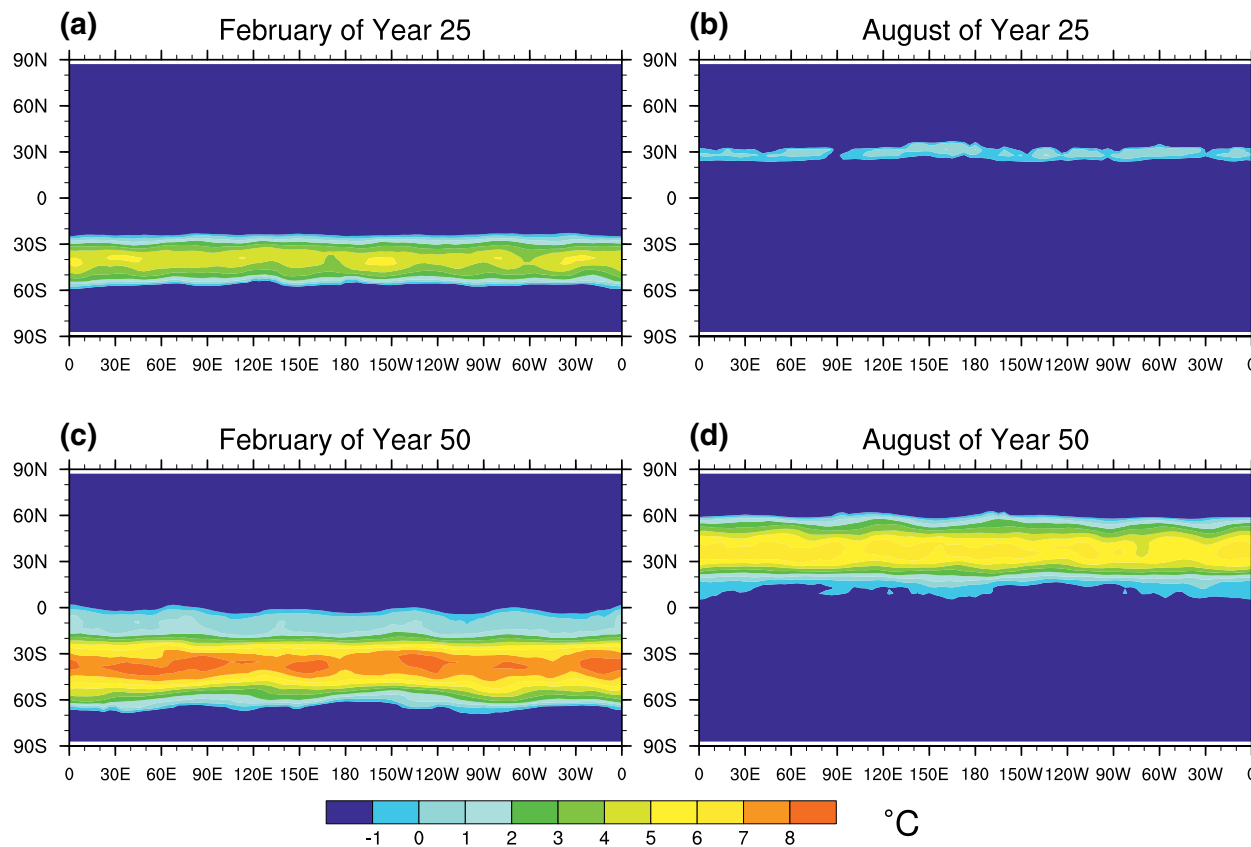


**Figure 13.** Distribution of temperature as a surrogate for implicit melt ponds in experiment IMP80. All regions with temperature greater than  $-1^{\circ}\text{C}$  (colors excluding the deep blue) can be approximately considered as having melt ponds.

For all the disintegration events around Antarctica, melt ponds or lakes formed by meltwater were observed prior to the disintegration. If fractures or crevasses exist on the ice surface, meltwater infilling will increase the tensile stress at the bottom tip of the fractures. If the tensile stress is greater than the fracture toughness of the ice, the fractures will then propagate downward and cut through the whole ice sheet. For this to happen, the initial fracture needs to be deep enough and the meltwater supply should be sufficient. Once it happens, it progresses quickly, normally within one melt season. The critical initial fracture depth was estimated for the Larsen B ice shelf to be 24–30 m if the upper limit for the fracture toughness ( $400 \text{ kPa m}^{1/2}$ ) is used (T. A. Scambos et al., 2000). Fractures or crevasses can also form near the grounding line where the continental ice sheets become afloat, and be advected away from the coastal region (T. A. Scambos et al., 2000). Therefore, we may expect that some crevasses exist, even in a snowball Earth.

If there are no pre-existing fractures, the meltwater, if deep enough, can induce cracking of ice by itself (Banwell et al., 2013). The meltwater normally gathers into discrete lakes on the ice surface. The lakes depress the ice sheet and rings of forebulges form around the lakes, where the tensile stress may be large enough to create fractures at the surface. Then infilling of water will make the cracks grow deeper and eventually cut through the ice. For an ice shelf of 200 m thick, the depth of lakes needs to be only a few meters deep to generate cracks (Banwell et al., 2013). The ice thickness in a snowball Earth is between 500 and 700 m near the equator when  $p\text{CO}_2$  is 0.1 bar (D. S. Abbot et al., 2013), the required water depth may thus be greater. This large thickness was likely an overestimate because a high surface albedo (0.6) was used in the study of D. S. Abbot et al. (2013) for demonstrative purpose. The overestimate was probably not severe because the annual mean surface temperature near the equator was only slightly lower than that calculated here in the experiment rd1, where no melt pond is allowed. Even if the ice was thick, it should not be a problem since the melt season of the equatorial region is all year long. The subtropical region, however, may not have a long enough melt season to induce cracks on the ice sheet.

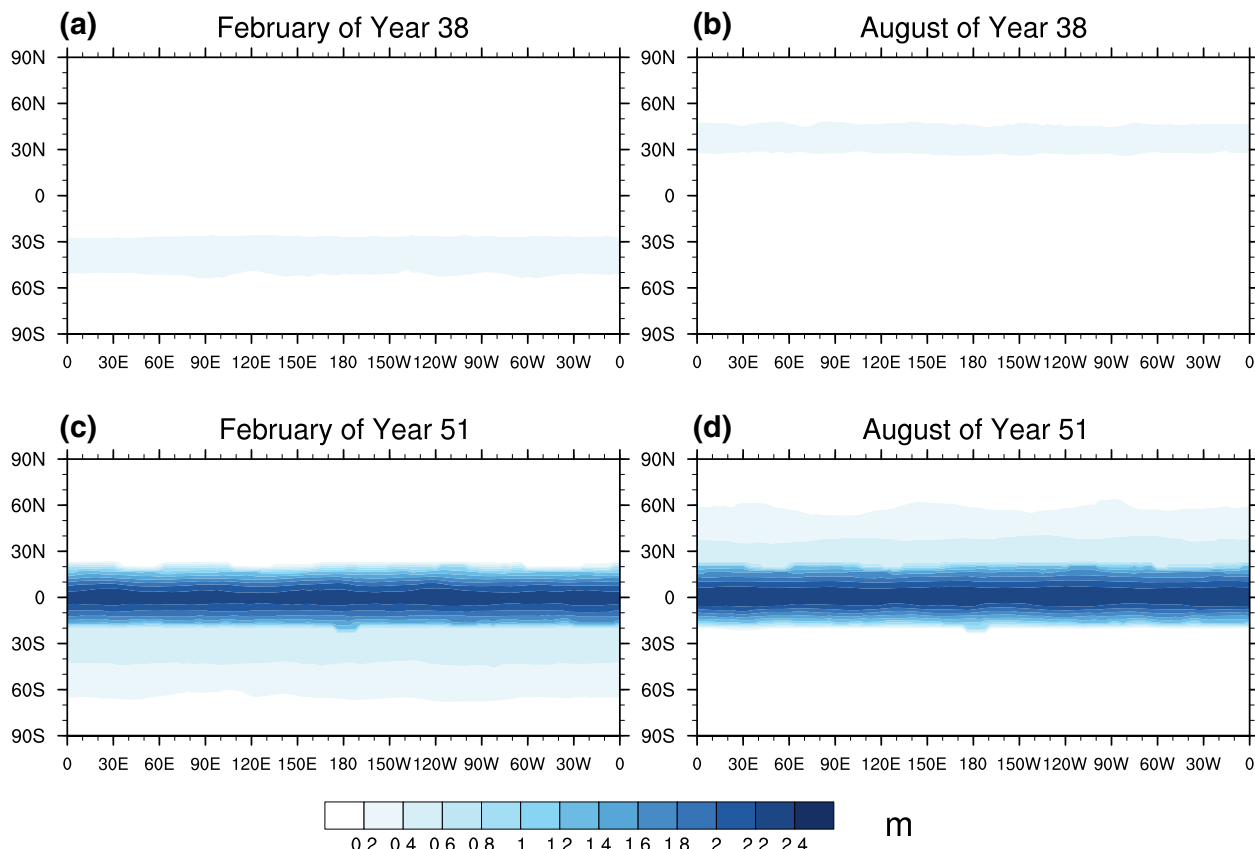


**Figure 14.** Distribution of thickness of meltwater in February and August in experiment EMP\_rd1. (a) and (b) are for model year 38, (c) and (d) are for model year 51.

Once the ice sheet is cut through by cracks, the meltwater on the surface will drain into the oceans beneath. The drainage of one lake induces a train of drainage events around itself. The drainage events induce more cracking of the ice sheet from the bottom (Banwell et al., 2013). The cracks may close up again when most of accumulated water is drained but the remnant cracks are weaker than other regions and will be easily reopened by next round of melt water accumulation. A question may be that when there is efficient drainage of surface melt water (as well as dust), can the tropical surface temperature remain high? Two sensitivity experiments, EMP\_rd1\_L5 and EMP\_rd1\_L2, are carried out to answer this question. In these experiments, the melt-water depth is limited to 0.5 m (EMP\_rd1\_L5) and 0.2 m (EMP\_rd1\_L2), respectively, to mimic the influence of drainage on surface water accumulation. It is assumed that the slushy surface ice and generally flat ice surface can always maintain some water, especially when there is continuous melting. Results show that the surface temperature indeed decreases, with the equatorial mean temperature decreases from 8°C (experiment EMP\_rd1) to 5 °C (EMP\_rd1\_L5) and 2°C (EMP\_rd1\_L2) (Figures 16a and 16b). These temperatures are still quite warm compared to that ( $\sim 10^\circ\text{C}$ ) experienced by Larson B ice shelf prior to its complete disintegration (Leeson et al., 2017). There is still significant rain almost everywhere (Figures 16c and 16d). Over the tropical region, the annual mean rain rate reaches  $\sim 2 \text{ mm/day}$  for the experiment EMP\_rd1\_L2 (the difference between blue curve and gray curve in Figures 16c and 16d gives rain rate). It indicates at least that the ice surface within the tropical region can maintain its wetness easily.

Next, we will speculate on how melt water production in the tropic region leads to the appearance of open ocean in four steps. First, there will be short cracks developing around discrete lakes and probably also deep rivers all over the ice surface (Figure 17a). Second, at some point, many small cracks may weaken the ice sheet enough so that long linear cracks may occur (called rifting; Figure 17b), similar to what happens on many disintegrating modern ice shelves (e.g. MacGregor et al., 2012). For modern ice shelves, the rifting occurs usually approximately along the edges. For a snowball Earth, there is no open ocean existing, thus

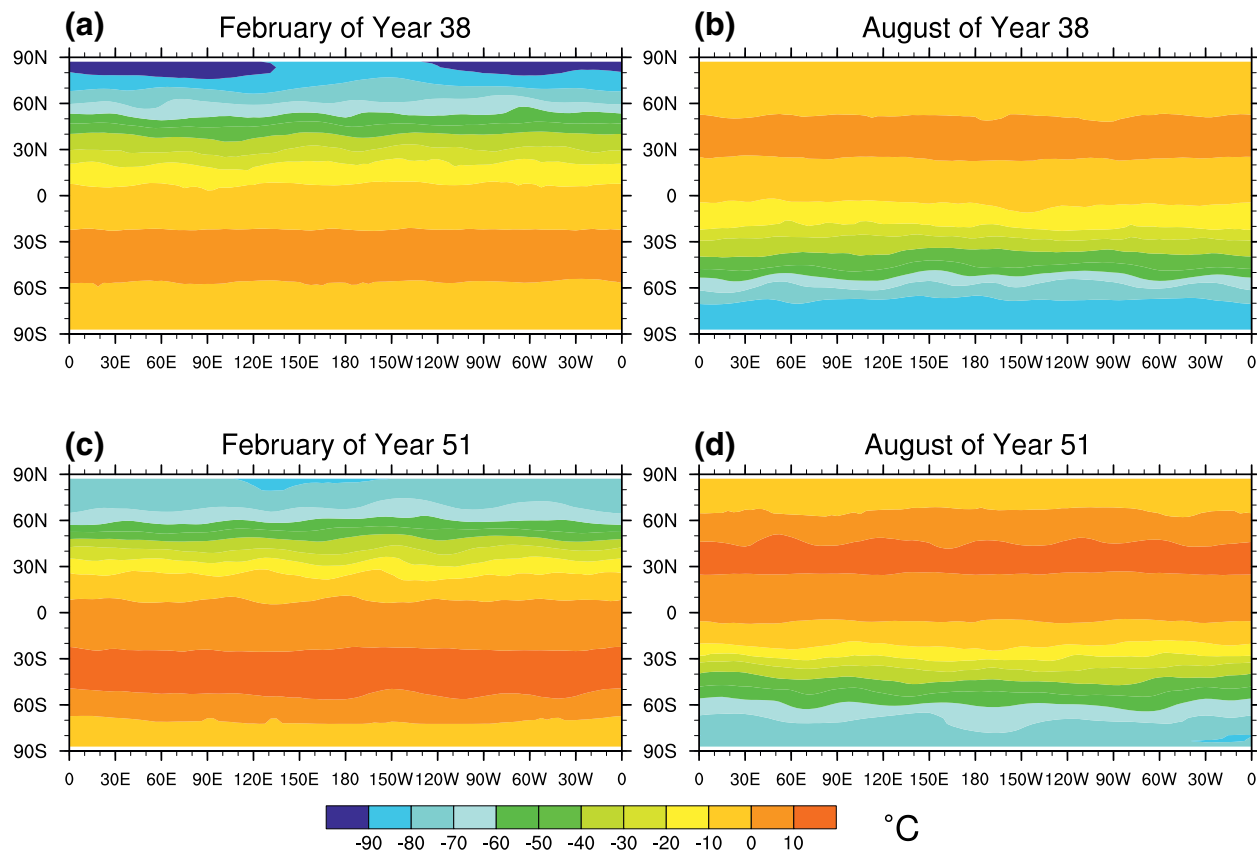


**Figure 15.** Similar to Figure 14 except here the surface temperature is shown.

no such edges. The tropical ice sheet is deforming under triaxial stresses, with the compressing stress along meridional direction. Rock experiments tell us that the rocks tend to fail at conjugate angles under triaxial stress, especially when the confining stress is similar in magnitude to the compressing stress (e.g. Z. Li et al., 2017). Therefore, large cracks might occur within the tropical region, oriented nearly 45° from the meridians (Figure 17b). As or even before the large cracks form, drainage of melt water may be sufficient enough so that large surficial lakes should disappear. The drainage of melt water also flushes dust into oceans, preventing thick dust layer to accumulate at the surface which may insulates the ice from melting on short timescales (e.g. seasonal).

The large cracks formed in the second stage may be especially stable due to the continuous action of the compressing stress from high-latitude ice sheets. They will also be maintained and widened by continuous flushing of melt water from surrounding area (Figure 17c). At the same time, the ice over tropical region thins due to continuous loss of surface mass. Once the large cracks are wide enough (e.g. a few hundred meters), the warming of ocean water within the cracks may become significant and start melting the ice from its lateral sides. As the cracks grow wider, calving may start to occur along these sides (Figure 17c). In the meantime, temperature in the tropical region increases substantially due to exposure of oceans. Intense melting occurs on the remaining ice sheets within the tropical region. These ice sheets might disintegrate abruptly into small pieces (Figure 17d), similar to what happened to the Larson B ice shelf at the Antarctic Peninsula.

It is difficult to give an estimate of the timescale for this whole process, i.e., from the start of melt pond appearance near equator to the appearance of large open ocean. An upper limit for the timescale may be given relatively easily. If there are no large stable cracks forming, we may not expect the positive feedback from the exposure of oceans. Then the ice sheet in the tropical region can only disappear by continuous surface melting. Figures 6d and 16c and 16d show that ~0.7 m or more of ice will be lost to evaporation alone every

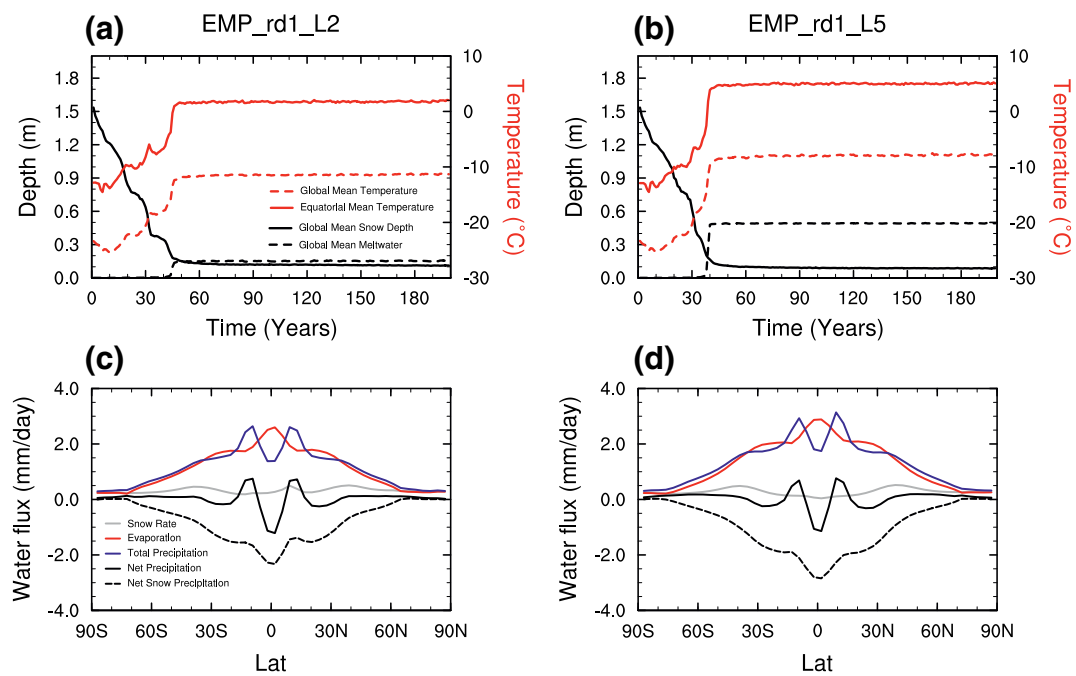


**Figure 16.** Results for Experiments EMP\_rd1\_L2 and EMP\_rd1\_L5 in which the melt-water depths are limited to 0.2 m (left) and 0.5 m (right), respectively. In the upper panels, the evolution of annual-mean surface temperature, snow depth, and thickness of melt water is shown; in the lower panels, zonal mean snow rate, precipitation rate, evaporation rate, net precipitation rate, and net accumulation rate (snow rate-evaporation rate) at the equilibrium state are shown. The equatorial region is roughly defined as between 6°S and 6°N.

year within the equatorial region. If ice loss of 0.3 m/yr (estimated from experiment EMP\_rd1\_L5) due to surface melting is added, this will give a timescale of  $\sim 500$  years if the initial ice thickness is 500 m. This timescale is certainly an overestimate because the marine ice in the deep layer that has a much lower albedo than the meteoric ice in the shallow layer (J. C. J. G. R. L. Goodman, 2006; Pollard & Kasting, 2005) will soon be exposed. The surface temperature will increase significantly and the speed of ice loss due to both evaporation and melting increases accordingly.

## 5. Conclusions

The deglaciation of a snowball Earth is studied by explicitly simulating the formation of melt ponds on thick sea-ice sheet. In previous studies, the start of the deglaciation of a snowball Earth is normally judged by looking at whether the annual mean surface temperature in the equatorial region reaches 0 °C. Our results show that this is not necessary; deglaciation will start when the annual mean equatorial surface temperature is only approximately  $-7.7^\circ\text{C}$  if formation of melt ponds are considered. At this temperature, the summer temperature in mid-latitude region is already high enough to form seasonal melt ponds. The formation of melt ponds provides a strong positive feedback and induces warming and melt ponds formation in the tropical region. The annual mean surface temperature within the equatorial region is increased substantially to  $6.1^\circ\text{C}$  in less than 10 years. Because surface temperature does not need to reach 0°C for deglaciation to start, the threshold  $p\text{CO}_2$  for snowball Earth deglaciation in previous studies was greatly overestimated. Taking the model used here as an example, the global mean surface temperature increases by  $\sim 3^\circ\text{C}$  for each doubling of  $\text{CO}_2$ , which means that the threshold  $\text{CO}_2$  could be overestimated by a factor of 4 if melt ponds are not considered. Our results also clearly demonstrate for the first time that although seasonal melt water appears first in the subtropical or mid-latitude regions, perennial melt water only appears near the equator. Deep ponds of melt water will form approximately  $\pm 15^\circ$  within the equator. We also provide a speculation on the processes through which the tropical sea glaciers are ablated after the equatorial ice starts to melt.

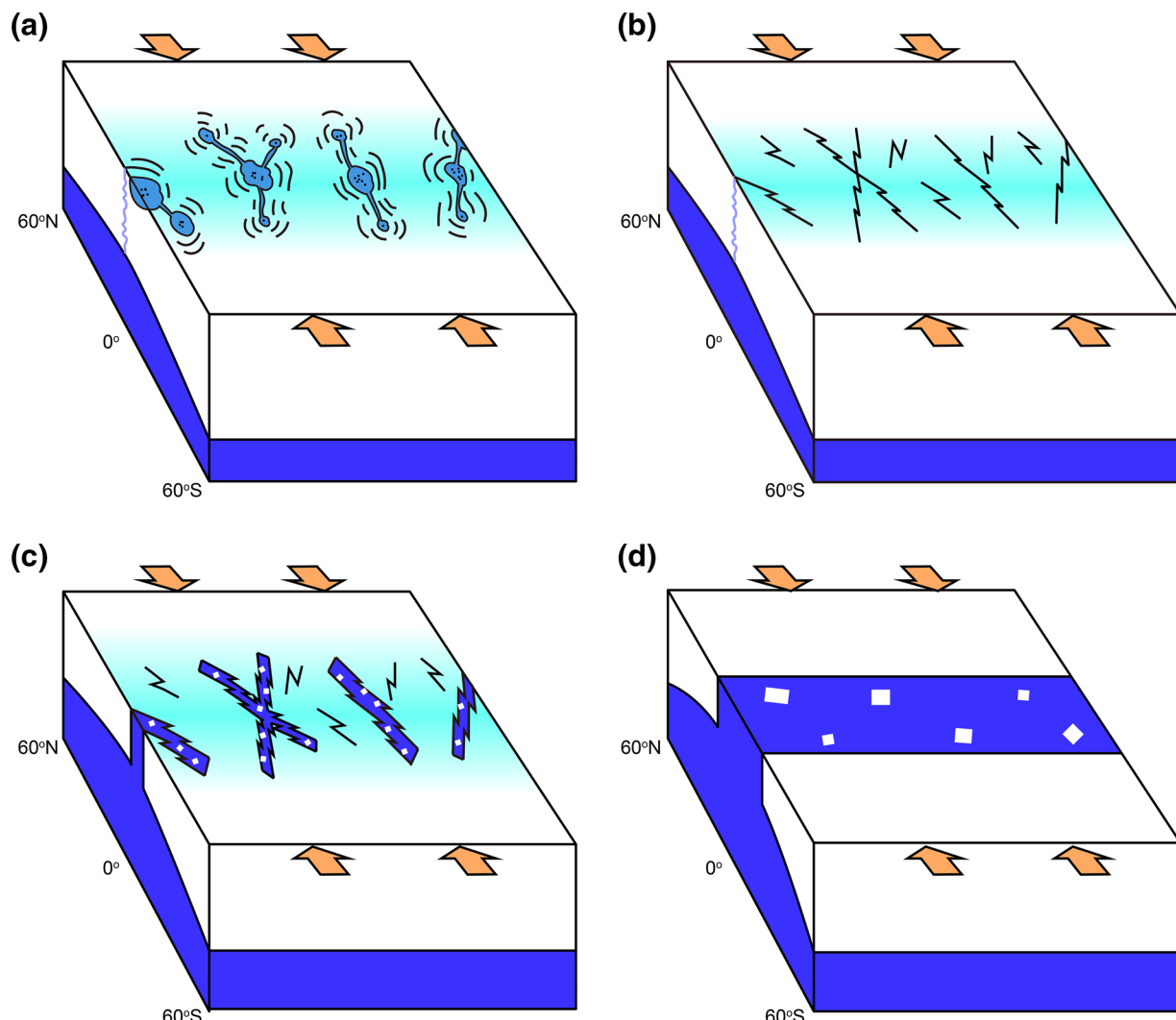


**Figure 17.** Schematics showing the ablation of tropical sea glacier in a snowball Earth. The white blocks are sea glaciers (thick sea ice) and deep blue represents seawater. The cyan color on the surface represents melt water, the deeper the color the deeper the water. In (a), the bluish ponds and belts represent large lakes and rivers, and the curved lines around them represent cracks formed due to the depression of the lakes and possibly deep rivers. Black dots indicate dust that has been flushed into the bottom of lakes. A moulin that cut through the ice is shown on the left. Note that there is no left or right boundary in a snowball Earth, only part of the longitudinal range is shown here for demonstrative purposes. In (b), both the long and short zigzags are rifts or cracks through which surface melt water is drained into the oceans so that no large lakes exist anymore. In (c), the long rifts widen due to continuous flushing of water and heating of ocean water. Calving starts to occur and the small white blocks are calved icebergs. The sea glacier also thins due to mass loss from continuous surface melting. In (d), the tropical sea glacier is completely calved. Orange arrows indicate the movement and compressional stresses from high-latitude glaciers.

## Data Availability Statement

The model results that support the findings of this study are available on Zenodo with the identifier <http://doi.org/10.5281/zenodo.4013203>.

## Acknowledgment

The simulations were done on the High-performance Computing Platform of Peking University. Y. Liu is supported by the National Natural Science Foundation of China under Grant 41875090 and 41761144072.

## References

- Abbot, D. S. (2014). Resolved snowball Earth clouds. *Journal of Climate*, 27(12), 4391–4402.
- Abbot, D. S., & Halevy, I. (2010). Dust aerosol important for snowball Earth deglaciation. *Journal of Climate*, 23(15), 4121–4132. <https://doi.org/10.1175/2010JCLI378.1>
- Abbot, D. S., & Pierrehumbert, R. T. (2010). Mudball: Surface dust and Snowball Earth deglaciation. *Journal of Geophysical Research*, 115, D03104. <https://doi.org/10.1029/2009jd012007>

- Abbot, D. S., Voigt, A., Branson, M., Pierrehumbert, R. T., Pollard, D., Le Hir, G., et al. (2012). Clouds and Snowball Earth Deglaciation. *Geophysical Research Letter*, 39(20), L20711. <https://doi.org/10.1029/2012GL052861>
- Abbot, D. S., Voigt, A., Li, D., Hir, G. L., Pierrehumbert, R. T., Branson, M., et al. (2013). Robust elements of Snowball Earth atmospheric circulation and oases for life. *Journal of Geophysical Research: Atmospheres*, 118(12), 6017–6027. <https://doi.org/10.1002/jgrd.50540>
- Ashkenazy, Y., Gildor, H., Losch, M., & Tziperman, E. (2014). Ocean circulation under globally glaciated Snowball Earth conditions: Steady-state solutions. *Journal of Physical Oceanography*, 44(1), 24–43.
- Axenrot, T., Ogonowski, M., Sandström, A., & Didrikas, T. (2009). Multifrequency discrimination of fish and mysids. *ICES Journal of Marine Science*, 66(6), 1106–1110.
- Banwell, A. F., MacAyeal, D. R., & Sergienko, O. V. (2013). Breakup of the Larsen B Ice Shelf triggered by chain reaction drainage of supraglacial lakes. *Geophysical Research Letters*, 40(22), 5872–5876. <https://doi.org/10.1002/2013GL057694>
- Bogorodsky, P., Marchenko, A., & Pnyushkov, A. (2006). *Thermodynamics of freezing melt ponds*. Paper presented at 18th IAHR International Symposium on Ice, Sapporo, Japan.
- Briegleb, B., Bitz, C., Hunke, E., Lipscomb, W., Holland, M., Schramm, J., et al. (2004). Scientific description of the sea ice component in the community climate system model. *Version*, 3, 70.
- Caldeira, K., & Kasting, J. F. (1992). Susceptibility of the early Earth to irreversible glaciation caused by carbon dioxide clouds. *Nature*, 359(6392), 226–228. <https://doi.org/10.1038/359226a0>
- Campbell, A. J., Waddington, E. D., & Warren, S. G. (2014). Refugium for surface life on Snowball Earth in a nearly enclosed sea? A numerical solution for sea-glacier invasion through a narrow strait. *Journal of Geophysical Research: Oceans*, 119(4), 2679–2690. <https://doi.org/10.1002/2013JC009703>
- Collins, W. D., Rasch, P. J., Boville, B. A., Hack, J. J., McCaa, J., Williamson, D. L., et al. (2004). *Description of the NCAR community atmosphere model (CAM 3.0)*, NCAR TECHNICAL NOTES, NCAR/TN-464+STR, 226.
- Eicken, H., Krouse, H. R., Kadko, D., & Perovich, D. K. (2002). Tracer studies of pathways and rates of meltwater transport through Arctic summer sea ice. *Journal of Geophysical Research*, 107(C10), 8046. <https://doi.org/10.1029/2000JC000583>
- Goodman, J. C. (2006). Through thick and thin: Marine and meteoric ice in a “Snowball Earth” climate. *Geophysical Research Letter*, 33(16), L16701. <https://doi.org/10.1029/2006GL026840>
- Goodman, J. C., & Pierrehumbert, R. T. (2003). Glacial flow of floating marine ice in “Snowball Earth”. *Journal of Geophysical Research*, 108(C10), 3308. <https://doi.org/10.1029/2002JC001471>
- Goodman, J. C., & Strom, D. C. (2013). Feedbacks in a coupled ice-atmosphere-dust model of the glacial Neoproterozoic “Mudball Earth”. *Journal of Geophysical Research: Atmospheres*, 118(20), 11546–11557. <https://doi.org/10.1002/jgrd.50849>
- Hoffman, P. F., Abbot, D. S., Ashkenazy, Y., Benn, D. I., Brocks, J. J., Cohen, P. A., et al. (2017). Snowball Earth climate dynamics and Cryogenian geology-geobiology. *Science Advances*, 3(11), e1600983.
- Hoffman, P. F., Kaufman, A. J., Halverson, G. P., & Schrag, D. P. (1998). A Neoproterozoic snowball earth. *Science*, 281(5381), 1342–1346.
- Hunke, E. C., Lipscomb, W. H., Turner, A. K., Jeffery, N., & Elliott, S. (2013). *CICE: The Los Alamos sea ice model documentation and software user's manual version 5.1* (Technical Report LA-CC-06-012). Los Alamos National Laboratory.
- Hu, Y., Yang, J., Ding, F., & Peltier, W. R. (2011). Model-dependence of the CO<sub>2</sub> threshold for melting the hard Snowball Earth. *Climate of the Past*, 7(1), 17–25.
- Le Hir, G., Donnadieu, Y., Krinner, G., & Ramstein, G. (2010). Toward the snowball earth deglaciation. *Climate Dynamics*, 35(2–3), 285–297. <https://doi.org/10.1007/S00382-010-0748-8>
- Le Hir, G., Ramstein, G., Donnadieu, Y., & Pierrehumbert, R. T. (2007). Investigating plausible mechanisms to trigger a deglaciation from a hard snowball Earth. *Comptes Rendus Geoscience*, 339(3–4), 274–287.
- Leeson, A. A., Van Wessem, J., Ligtenberg, S., Shepherd, A., Van Den Broeke, M., Killick, R., et al. (2017). Regional climate of the Larsen B embayment 1980–2014. *Journal of Glaciology*, 63(240), 683–690. <https://doi.org/10.1017/jog.2017.39>
- Li, D., & Pierrehumbert, R. T. (2011). Sea glacier flow and dust transport on Snowball Earth. *Geophysical Research Letters*, 38(17), L17501. <https://doi.org/10.1029/2011GL048991>
- Li, Z., Shi, J., Tang, A. (2017). An investigation of failure modes and failure criteria of rock in complex stress states. *Journal of the Southern African Institute of Mining and Metallurgy*, 117(3), 245–255.
- Liu, Y., Yang, J., Bao, H., Shen, B., & Hu, Y. (2020). Large equatorial seasonal cycle during Marinoan snowball Earth. *Science Advances*, 6(23), eaay2471.
- MacGregor, J. A., Catania, G. A., Markowski, M. S., & Andrews, A. G. (2012). Widespread rifting and retreat of ice-shelf margins in the eastern Amundsen Sea Embayment between 1972 and 2011. *Journal of Glaciology*, 58(209), 458–466.
- Oleson, K. W., Dai, Y., Bonan, G. B., Bosilovich, M., Dickinson, R., Dirmeyer, P., et al. (2004). *Technical description of the community land model (CLM)*, NCAR Technical Note, NCAR/TN-495+STR, 174. <https://doi.org/10.5065/D6N877R0>
- Paterson, W. S. B. (1994). *Physics of Glaciers*. Butterworth-Heinemann.
- Petrich, C., Eicken, H., Polashenski, C. M., Sturm, M., Harbeck, J. P., Perovich, D. K., et al. (2012). Snow dunes: A controlling factor of melt pond distribution on Arctic sea ice. *Journal of Geophysical Research*, 117(C9), C09029. <https://doi.org/10.1029/2012JC008192>
- Pierrehumbert, R. T. (2004). High levels of atmospheric carbon dioxide necessary for the termination of global glaciation. *Nature*, 429(6992), 646–649. <https://doi.org/10.1038/nature02640>
- Pierrehumbert, R. T. (2005). Climate dynamics of a hard snowball Earth. *Journal of Geophysical Research*, 110(D1), D01111. <https://doi.org/10.1029/2004JD005162>
- Pierrehumbert, R., Abbot, D., Voigt, A., Koll, D. (2011). Climate of the neoproterozoic. *Annual Review of Earth and Planetary Sciences*, 39, 417–460. <https://doi.org/10.1146/annurev-earth-040809-152447>
- Polashenski, C., Perovich, D., & Courville, Z. (2012). The mechanisms of sea ice melt pond formation and evolution. *Journal of Geophysical Research*, 117, C01001. <https://doi.org/10.1029/2011JC007231>
- Pollard, D., & Kasting, J. F. (2005). Snowball Earth: A thin-ice solution with flowing sea glaciers. *Journal of Geophysical Research*, 110(C7), C07010. <https://doi.org/10.1029/2004JC002525>
- Richter-Menge, J. A., Perovich, D. K., & Pegau, W. S. (2001). Summer ice dynamics during SHEBA and its effect on the ocean heat content. *Annals of Glaciology*, 33(1), 201–206. <https://doi.org/10.3189/172756401781818176>
- Roeckner, E., Mauritsen, T., Esch, M., & Brokopf, R. (2012). Impact of melt ponds on Arctic sea ice in past and future climates as simulated by MPI-ESM. *Journal of Advances in Modeling Earth Systems*, 4(3), M00A02. <https://doi.org/10.1029/2012MS000157>
- Ross, S. M. (2010). *A first course in probability*. Pearson Prentice Hall.

- Scambos, T., Fricker, H. A., Liu, C.-C., Bohlander, J., Fastook, J., Sargent, A., et al. (2009). Ice shelf disintegration by plate bending and hydro-fracture: Satellite observations and model results of the 2008 Wilkins ice shelf break-ups. *Earth and Planetary Science Letters*, 280(1–4), 51–60.
- Scambos, T. A., Hulbe, C., Fahnestock, M., & Bohlander, J. (2000). The link between climate warming and break-up of ice shelves in the Antarctic Peninsula. *Journal of Glaciology*, 46(154), 516–530.
- Scharien, R., Hochheim, K., Landy, J., & Barber, D. (2014). Sea ice melt pond fraction estimation from dual-polarisation C-band SAR-Part 2: Scaling in situ to Radarsat-2. *TCD*, 8(1), 845–885.
- Schwarz, G., Frenzel, W., Richter, W. M., Täuscher, L., & Kubsch, G. (2016). A multidisciplinary science summer camp for students with emphasis on environmental and analytical chemistry. *Journal of Chemical Education*, 93(4), 626–632.
- Shepherd, A., Wingham, D., Payne, T., & Skvarca, P. (2003). Larsen ice shelf has progressively thinned. *Science*, 302(5646), 856–859.
- Stepanenko, V. M., Goyette, S., Martynov, A., Perroud, M., Fang, X., & Mironov, D. (2010). *First steps of a Lake Model Intercomparison Project*. LakeMIP.
- Tajika, E. (2003). Faint young sun and the carbon cycle: Implication for the proterozoic global glaciations. *Earth and Planetary Science Letters*, 214(3–4), 443–453.
- Taylor, P., & Feltham, D. (2004). A model of melt pond evolution on sea ice. *Journal of Geophysical Research*, 109(C12), C12007. <https://doi.org/10.1029/2004JC002361>
- Tziperman, E., Abbot, D. S., Ashkenazy, Y., Gildor, H., Pollard, D., Schoof, C. G., et al. (2012). Continental constriction and oceanic ice-cover thickness in a Snowball-Earth scenario. *Journal of Geophysical Research*, 117(C5), C05016. <https://doi.org/10.1029/2011JC007730>
- Webster, M., Gerland, S., Holland, M., Hunke, E., Kwok, R., Lecomte, O., et al. (2018). Snow in the changing sea-ice systems. *Nature Climate Change*, 8(11), 946–953.